Jussi Nieminen

# Brain activation in a complex stimulus

**Faculty of Electronics, Communications and Automation**

Thesis submitted for examination for the degree of Master of Science in Technology.
12.4.2010

**Thesis supervisor and instructor:**

Prof. Jouko Lampinen

Aalto University
School of Science
and Technology

AALTO-YLIOPISTO
TEKNILLINEN KORKEAKOULU

DIPLOMITYÖN
TIIVISTELMÄ

Tekijä: Jussi Nieminen

Työn nimi: Aivoaktivaatio monimuotoisessa ärsykkeessä

Päivämäärä: 12.4.2010 Kieli: Englanti Sivumäärä:7+47

Elektroniikan, tietoliikenteen ja automaation tiedekunta

Lääketieteellisen tekniikan ja laskennallisen tieteen laitos

Professuuri: Laskennallinen tekniikka Koodi: S-114

Valvoja ja ohjaaja: Prof. Jouko Lampinen

Tutkimuksessa luonnollisia olosuhteita jäljitellään näyttämällä elokuvaa. Tällaisen ärsykkeen aiheuttamaa yleistä aivoaktivaatiota tutkitaan. Aivojen vasteita kyseiselle ärsykkeelle selvitetään. Riippumattomien komponenttien analyysia (ICA) ja koehenkilöiden välisiä korrelaatioita (ISC) käytetään datan analysointiin. ICA:sta saatujen komponenttien konsistenssia ja vaihtelevuutta testataan. Koehenkilöiden samankaltaisuutta tutkitaan ISC:lla. Stabiilimmat komponenttit aiheuttavia ärsykkeitä etsitään elokuvasta, kuten tehdään myös joidenkin aivoalueiden ISC:lla.

Elokuva Tulitikkutehtaan tyttö näytettiin koehenkilöille, joiden aivojen aktiivisuutta mitattiin toiminnallisella magneettikuvauksella (fMRI). Koehenkilöt saivat vapaasti katsoa elokuvaa eikä erillisiä ohjeita annettu. FMRI:sta saatu data analysoitiin ryhmä ISC:lla ja ICA:lla. ICA:n stabiilisuutta ja konsistenssia testattiin ajamalla useita bootstrap ICA:ja. ISC laskettiin koko elokuvalle ja ikkunoidulle datalle erikseen. Koko elokuva jaettiin viiteen taajuuskaistaan eri taajuuksien korrelaatioiden vertailua varten.

ICA paljasti stabiileja komponentteja kuuloa ja näköä prosessoivilla alueilla sekä parietaali alueella. ISC näytti synkronisaatiota pääosin samoilla alueilla. Datan jako taajuuskaistoihin paljasti ääni ja kuulo alueiden hallinnan korkeilla taajuuksilla. Aivojen etuosissa oli korrelaatiota matalilla taajuuksilla.

Avainsanat: fMRI, ICA, konsistenssi, ISC

Aalto University
School of Science and Technology

abstract of the
master's thesis

Author: Jussi Nieminen

Title: Brain activation in a complex stimulus

Date: 12.4.2010 Language: English Number of pages:7+47

Faculty of Electronics, Communications and Automation

Department of Biomedical Engineering and Computational Science

Professorship: Computational engineering Code: S-114

Supervisor and instructor: Prof. Jouko Lampinen

Natural conditions are imitated by showing a movie as a stimulus. The common brain activity caused by this kind of stimulus is studied. The interest is to find what kind of responses brain gives to the stimulus. The independent component analysis (ICA) and the intersubject correlation (ISC) are used to analyze the data. Consistency and variability of the components revealed by group ICA are tested. Similarities between the subjects are tested by ISC. The stimuli causing the most consistent components are traced from the movie as is also done with ISC in certain brain regions.

The beginning of the movie Tulitikkutehtaan tyttö was shown to subjects whose brain activity was recorded with functional magnetic resonance imaging (fMRI). The subjects could freely view the movie and no instructions were given. The resulting data from fMRI was analyzed by group intersubject correlation and independent component analysis. The stability and the consistency of ICA was tested by bootstrapping the data. Intersubject correlation was calculated to the whole movie and windowed data separately. The whole movie was also divided to 5 subbands to compare correlations in different frequencies.

ICA revealed stable components in the auditory and the visual processing areas and in the parietal area. ISC showed synchronization mainly in the same regions. The subbands showed the dominance of the auditory and the visual processing areas in high frequencies. Frontal part of the brain had correlation in low frequencies.

Keywords: fMRI, ICA, consistency, ISC

# Preface

This work was done at the department of Biomedical Engineering and Computational Science in Aalto University School of Science and Technology. I would like to thank my supervisor Professor Jouko Lampinen for the possibility to work in this project. I am grateful to Mikko Sams, Iiro Jääskeläinen, Juha Salmitaival, Juha Lahnakoski, Jukka-Pekka Kauppi and Jussi Tohka for supporting me in the study. Finally, I wish to thank all my coworkers, family and friends.

Otaniemi, 21.1.2008

Jussi Nieminen

# Contents

# Symbols and appriviations

## Symbols

| | |
|---|---|
| $w_0$ | Larmor frequency |
| $\gamma$ | gyromagnetic ratio |
| $B_0$ | external magnetic field |
| $M_0$ | net magnetization |
| $\alpha_f$ | flip angle |
| $B_1$ | strength of the RF pulse |
| $t_p$ | duration of the pulse |
| $G$ | gradient field |
| $B$ | magnetic field |
| $S(t)$ | MR signal measured by an antenna |
| $T$ | relaxation time |
| $k(t)$ | k-space |
| $S(x, y)$ | intensity in a pixel |
| $f(x, y, z)$ | three dimensional Gaussian kernel |
| $x$ | random vector of the observed values |
| $a$ | attenuation |
| $s$ | random vector of the sources |
| $A$ | mixing matrix |
| $z$ | observed value |
| $W$ | inverse of the mixing matrix |
| $\Sigma_i$ | noise covariance matrix |
| $\sigma^2$ | covariance |
| $R_x$ | covariance matrix |
| $X$ | voxel-wise prewhitened data |
| $p$ | number of observations |
| $q$ | number of sources |
| $Q$ | square matrix |
| $\nu$ | Gaussian variable of zero mean and unit variance |
| $F$ | nonquadratic function |
| $\pi$ | coefficient |
| $\mu$ | mean |
| $\sigma$ | variance |
| $r$ | correlation |
| $\alpha$ | threshold |
| $p$ | probability |
| $V$ | number of true null hypothesis |
| $p_i$ | p-value of the test i |
| $C$ | correlation matrix |
| $k$ | threshold value |
| $d$ | longest acceptable path |

## Appriviations

| | |
|---|---|
| MRI | magnetic resonance imaging |
| fMRI | functional magnetic resonance imaging |
| NMR | nuclear magnetic resonance |
| ICA | independent component analysis |
| ISC | intersubject correlation |
| GISC | group intersubject correlation |
| RF | radio frequency |
| FID | free induction decay |
| TR | repetition time |
| GE | gradient echo |
| SE | spin echo |
| TE | echo time |
| BOLD | blood oxygenation level dependent |
| HDR | hemodynamic response |
| EPI | echo planar imaging |
| DOF | degrees of freedom |
| MNI | Montreal neurological institute |
| PICA | probabilistic independent component analysis |
| PCA | principal component analysis |
| ALS | alternating least squares |
| FWE | familywise error rate |
| FDR | false discovery rate |

# 1 Introduction

The brain is one of human's most important organs. Many studies for understanding how the brain works have been done over last decades. The brain controls almost every part of the human body. Actually the brain commands our everyday movements and behavior. The interest of understanding functions of the brain is therefore understandable.

Brain's responses to outside stimuli have been studied in different ways. Earlier the stimuli have been simple sounds or pictures. These very controlled studies have showed which regions of the brain corresponds to auditory, visual or memory related stimuli. Nowadays studies have moved towards more naturalistic stimuli where the stimuli are related more closely to everyday life. This way it is possible to model brain in everyday events. One of the novel approaches is called neurocinematics. In neurocinematics a movie is presented as a stimulus which is clearly more natural than still pictures or beep sounds.

New techniques for observing brain activity has been developed allowing the use of better methods in brain studies. In functional magnetic resonance imaging (fMRI) changes in blood oxygenation level are measured revealing which regions of the brain are active at a particular time point. Images can be taken at 2 second intervals revealing accurately the changes in the brain.

The object of the study is to find brain responses common to most of the subjects. The consistency of independent component analysis (ICA) is tested and stimuli causing the consistent components are tried to be found from the movie. Correlations between subjects during the movie watching are calculated to find which regions have synchronization. To recognize the stimuli in the movie the correlations are also calculated in shorter clips. Besides the study better understanding of the used methods should be achieved which can be utilized in forthcoming studies.

Experiment's setup corresponds to the studies of Hasson et al.[1], Bartels and Zeki[2] and Jääskeläinen et al.[3] where they viewed a movie that subjects could freely watch. A movie Tulitikkutehtaan tyttö is shown to 12 subjects whose brain activity is recorded with fMRI. The resulting data is analyzed by the intersubject correlation (ISC) and the independent component analysis (ICA). The stability and consistency of ICA is tested by bootstrapping the data. The results of ICA and ISC are also compared.

The intersubject correlation is counted for every subject pair. One common value is formed from the subjects' correlations. The data is divided to 5 subbands and it is also windowed to 71 clips. The synchronizations are counted for the whole data in every band separately and in full band for the windowed data.

Hypothesis is that the auditory and the visual processing areas of the brain have strong correlations over the whole movie in full band. These areas should also dominate in higher frequencies where frontal areas should have correlation only in lower frequencies. The correlations in different parts of the brain at different time points are expected to be found as the auditory processing areas should be active when there is speech in the movie and the visual processing areas should have higher activation during visual stimuli.

The consistency of the found independent components is examined by bootstrapping group ICA. Also spatial and temporal variability of the independent components are examined. Here it is assumed that some very stable components caused by the real stimuli and some artifacts will be found. Finally these two methods to analyze fMRI are compared and their advantages and disadvantages are discussed.

In Chapter 2 the basics of the functional magnetic resonance imaging are gone through. Also preprocessing steps for fMRI data are introduced and two analysis methods the independent component analysis and the intersubject correlation are explained. Finally previous studies are discussed. The experiment setup and the used analysis methods are explained Chapter 3. The results of ICA and ISC are presented in Chapter 4. Chapter 5 contains the discussion of the study.

# 2 Theory

## 2.1 MRI

Magnetic Resonance Imaging (MRI) is a medical imaging technique which produces high quality images of the human body. It is used in neurological, oncological and musculoskeletal studies. MRI is based on nuclear magnetic resonance (NMR), which was first discovered in 1945 by Edward Purcell and independently by Felix Bloch and Robert Pound. The first MR image was published in 1973.[4]

### 2.1.1 Definition of MRI

In MRI the interests are nuclei in human body. Nuclei consist of protons and neurons. Often a hydrogen atom is used in MRI because it is abundant in all tissue types. Its nucleus consists of one positively charged proton. A proton spins on its own axis generating a magnetic field known as magnetic moment. The spinning behavior of the hydrogen atom is quite simple compared to heavier atoms which favors its use in MRI.[4]

In addition to the spinning nuclei a strong magnetic field is needed to perform MRI. This magnetic field affects the hydrogen nuclei in human body. Normally nuclei are randomly aligned. When a strong magnetic field is generated the nuclei align about with the direction of the field. They still experience torque which makes them precess around direction of the external magnetic field. This is called Larmor precession. It is proportional to the magnetic field given as Larmor frequency

$$w_0 = \gamma B_0 \tag{1}$$

where $\gamma$ is the gyromagnetic ratio and $B_0$ is the external magnetic field.[4]

Protons can align parallel or anti-parallel in the field neutralizing each other. Still the parallel state is slightly favored. The magnetic moment vectors are evenly spread out because the protons are all out of phase with each other. The sum of all magnetic moments is aligned exactly with the main field $B_0$ and it is called the net magnetization $M_0$.[4]

$M_0$ is much smaller ($1\mu T$) than $B_0$ ($1T$) so it can not be yet measured. To measure $M_0$ a $90^o$ radio frequency (RF) pulse is used. RF frequency must be the Larmor frequency. $M_0$ moves away from $B_0$ as long as RF is switched on. The flip angle will be

$$\alpha_f = \gamma B_1 t_p \tag{2}$$

where $B_1$ is the strength of the RF pulse and $t_p$ is duration of the pulse. RF signal also brings all the spins into phase coherence.

After the RF pulse $M_0$ is measured by detecting the voltage it induces in a receiver coil. The coil sees a magnetic field which induces a voltage varying at the Larmor frequency. The signal is called Free Induction Decay (FID). FID is never measured directly instead echoes are created and measured. Right after RF pulse is switched off nuclei realign their $M_0$ so that it is parallel to $B_0$. This measurement

is processed to obtain MR images. The time between two excitation pulses is called repetition time (TR).[4]

There are two types of echoes gradient (GE) and spin echoes (SE). In GE the excitation pulse is used to create a smaller flip angle $\alpha_f$ than 90 degrees. A negative gradient lobe is applied right after the excitation pulse causing rapid dephasing of the transverse magnetization. Then a positive gradient is applied which reverses the magnetic field gradient. After a certain time gradients will come back into the same phase making a gradient echo. This time is called echo time (TE). In SE spins are left to dephase a certain time after a 90 degree RF pulse. After a time T a 180 degree pulse is used to flip the spins around their axes. All the spins will come back to the starting phase creating the spin echo. This will happen at time 2T after the first RF pulse. The spin echo is illustrated in figure(1).[4]

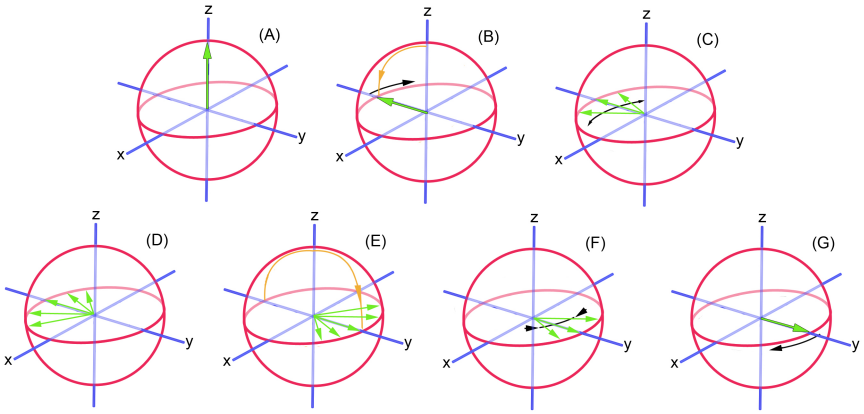


Figure 1: SE where in B a 90 degree pulse is applied and in E a 180 degree pulse flips the spins[5]

When the RF signal is switched off protons start to realign back to their equilibrium position. This is called relaxation time. The protons lose energy that they absorbed from the pulse during the relaxation. $M_0$ parallel to $B_0$ starts to recover and it is called $T_1$ recovery. The time when $M_0$ has recovered 63% of its equilibrium value is called the relaxation time $T_1$. Also a dephasing of the spins following their phase coherence happens during this time. The vector sum of the magnetic moments and also the measured FID decay. This process is called the spin-spin relaxation. The time when the transverse magnetization drops to 37% of it initial value is the spin-spin relaxation time $T_2$. In human body $T_1$ always takes longer time than $T_2$.[4]

An image still cannot be created from a MR signal detected by the static magnetic field and the radio frequency coil. Gradient coils are used to get the spatial information needed for constructing MRI. A gradient coil causes the MR signal to become spatially dependent. The coil changes the main magnetic field so that its strength differs at different locations. A magnetic field that increases in a spatial direction is created by a gradient coil making the recovery of the spatial information easy. The spatial directions x and y are going perpendicularly and z parallel to the main field.[6]

The Bloch equation describes the change in the net magnetization

$$\frac{dM}{dt} = \gamma M \times B + \frac{1}{T_1}(M_0 - M_z) - \frac{1}{T_2}(M_x - M_y). \tag{3}$$

The longitudinal magnetization

$$M_z(t) = M_0(1 - e^{-t/T_1}) \tag{4}$$

and the transverse magnetization

$$M_{xy}(t) = M_x(t) + M_y(t)i = M_{xy0}e^{-t/T_2}e^{-iwt} \tag{5}$$

can be calculated from the Bloch equation where

$$M_x(t) = -M_0 e^{-t/T_2} \cos wt \tag{6}$$

$$M_y(t) = M_0 e^{-t/T_2} \sin wt. \tag{7}$$

Now the magnetic field depends on the static field $B_0$ and the gradient fields $G$.

$$B(t) = B_0 + G_x(t)x + G_y(t)y + G_z(t)z \tag{8}$$

The MR signal measured by an antenna can be expressed as the summation of signal from every voxel

$$S(t) = \int_x \int_y \int_z M_{xy0}(x, y, z)e^{-t/T_2}e^{-iw_0 t}e^{-i\gamma \int_0^t G_x(t)x + G_y(t)y + G_z(t)z dt} dxdydz. \tag{9}$$

Modern scanners demodulate the detected signal with the resonance frequency $w_0$ so term $e^{-iw_0 t}$ can be removed. Also term $e^{-t/T_2}$ can be removed because it does not affect the signals spatial location only the magnitude.[6]

Often 2D-imaging is used where the $G_z$ gradient and the excitation pulse are simultaneously applied allowing selection of the defined slice. Only the spins in the slice are tuned to match the frequency of the excitation pulse. Interleaved slice acquisition, where for example 10 slices are excited in order 1, 3, 5, 7, 9, 2, 4, 6, 8, 10, is used to avoid the effect of the previous excitation pulse. The magnetization of an individual voxel within a slice is

$$M(x, y) = \int_{z_0 - \triangle z/2}^{z_0 + \triangle z/2} M_{xy0}(x, y, z)dz \tag{10}$$

where $z_0$ is the centre of the plain. After the slice selection the magnetization is dependent only on x and y. A spatial frequency space the k-space is adopted to make it easier to understand the relation between $S(t)$ and the object to be imaged $M(x, y)$. A transform

$$k_x(t) = \frac{\gamma}{2\pi} \int_0^t G_x(\tau)d\tau \tag{11}$$

$$k_y(t) = \frac{\gamma}{2\pi} \int_0^t G_y(\tau) d\tau \tag{12}$$

is applied. The MR signal from equation (9) becomes

$$S(t) = \int_x \int_y M(x,y) e^{-i2\pi k_x(t)x} e^{-i2\pi k_y(t)y} dxdy. \tag{13}$$

The gradients $G_x$ and $G_y$ are applied for encoding of the spatial locations. Every voxel in the slice gets a unique frequency. The transverse magnetization is represented in the k-space. $G_y$ is turned on before the data acquisition accumulating a certain amount of phase offset. During the data acquisition $G_x$ is turned on changing the frequencies of the spins. Each voxel is collected in a slightly different time point. Collection of the data is called filling the k-space. Finally the MR image is reconstructed from the k-space using the inverse Fourier transform. Also 3D-imaging is used mostly in anatomical scans. There two phase gradients and one frequency gradient are used.[6]

### 2.1.2 Images

MR images are produced using pulse sequences. The sequence contains radiofrequency pulses and gradient pulses. Images are named depending on which $T_1$ or $T_2$ relaxation time is used. Here are few images listed.[4]

#### $T_1$-weighted MRI

GE or SE signal is used in $T_1$-weighted MRI with short TE and TR. Scan can be run very fast due the short repetition time TR. $T_1$- weighted images have a good contrast. They are usually used as anatomy pictures because different tissues are distinguished clearly. Fat is bright, water is grey and fluids are dark.[4]

#### $T_2$-weighted MRI

SE is used in $T_2$-weighted MRI. SE has long TE and TR. Here fluids are bright and water- and fat-based tissues are darker.[4]

#### $T_2$*-weighted MRI

In $T_2$*-weighted MRI scans GE sequence is used with long TE and TR. This increases contrast when measuring venous blood. Fluids are bright and other tissues are grey in $T_2$*-images.[4]

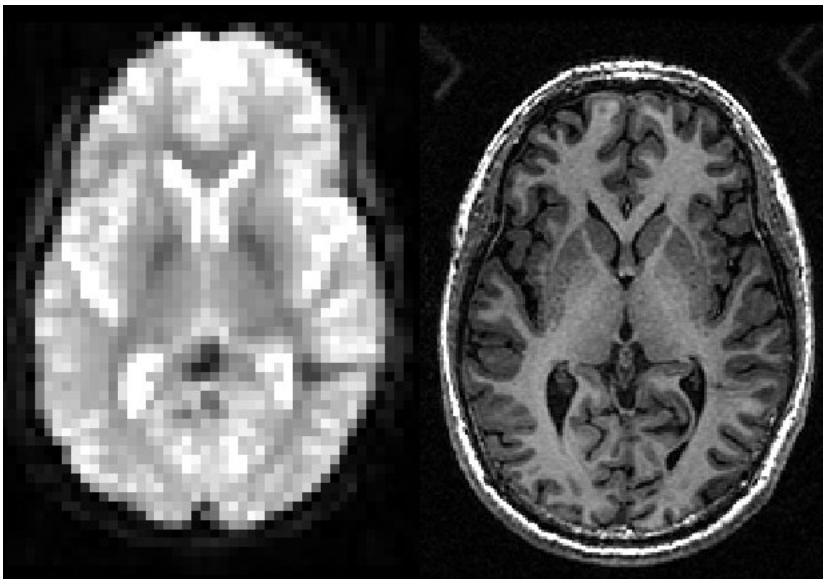

Figure 2: The $T_2$*-weighted image on the left and the $T_1$-weighted image on the right

### 2.1.3 BOLD fMRI

The blood oxygenation level dependent (BOLD) functional MRI is a MRI method which measures the level of blood oxygen in different parts of the brain. It is based on different magnetic properties of deoxygenated and oxygenated hemoglobin. Deoxygenated hemoglobin is paramagnetic while oxygenated hemoglobin is diamagnetic. When a human detects a stimulus it causes neural activity in his brain. An active neuron uses more energy than an inactive neuron. The need of energy causes an increase of blood flow that delivers the primary energy sources glucose and oxygen to the active neurons.[6]

T2*-imaging is used in BOLD fMRI. Introduction of an object with magnetic susceptibility into a magnetic field causes spin dephasing. This will result decay in the transverse magnetization which depends on T2*. High oxygenated blood should show more MR signal and low oxygenated blood should show less. These differences and changes can be measured by MR imaging. The change in MR signal caused by neural activity is called the hemodynamic response (HDR). There is a lag in HDR compared to the neuronal events. As neuronal responses occur in tens of milliseconds HDR can be seen in 3-6 seconds.[6]

After the neural activity there is lack of oxygen because it is extracted by the active neurons. This causes an increased inflow of oxygenated blood. More oxygenated blood is supplied than is extracted decreasing the amount of deoxygenated hemoglobin in blood causing a decrease in signal loss due the T2* effect. When monitoring an active voxel by BOLD fMRI increase of neural activity can be seen after 2 seconds and the peak of activity is reached in about 5 seconds. After the peak signal decreases below the baseline and remains there a short period of time. This is

known as the poststimulus undershoot. If multiple consecutive stimuli happen the amplitude of the BOLD signal remains higher during the stimuli.[6]

BOLD fMRI is used to study quick changes in the brain. It is applied in cognitive neuroscience in defining networks, understanding mechanisms and finding the correlation between brain and behavior. It can be helpful in medical science in mapping damaged areas of the brain and testing drugs.[7]

### 2.1.4 EPI

Understanding the function of the brain requires fast acquirement of the images. In the echo planar imaging (EPI) the k-space is filled using a single excitation and rapid gradients[6]. EPI is a fast method to form a complete image from a single data sample. The data is collected to the k-space and after that transformed to an image by Fourier-transform. The 3D-image is collected one slice at the time. In EPI first a RF signal is sent. After RF signal a read signal and a phase signal are sent. This is illustrated in figure(3) where the k-space is covered in two segments and $G_x$ is the read signal and $G_y$ is a phase signal. The k-space can also be covered in more segments. EPI basically reads one row at a time and then jumps to a next row. This is illustrated in figure(4), where a two shot interleaved EPI is used.[7]

These images usually have poor resolution because of the small acquisition time required. Their anatomical contrast is also poor because they are tuned to highlight physiological changes. These images can be taken in less than one second and are therefore suitable for fMRI when blood oxygen changes are monitored.[8]

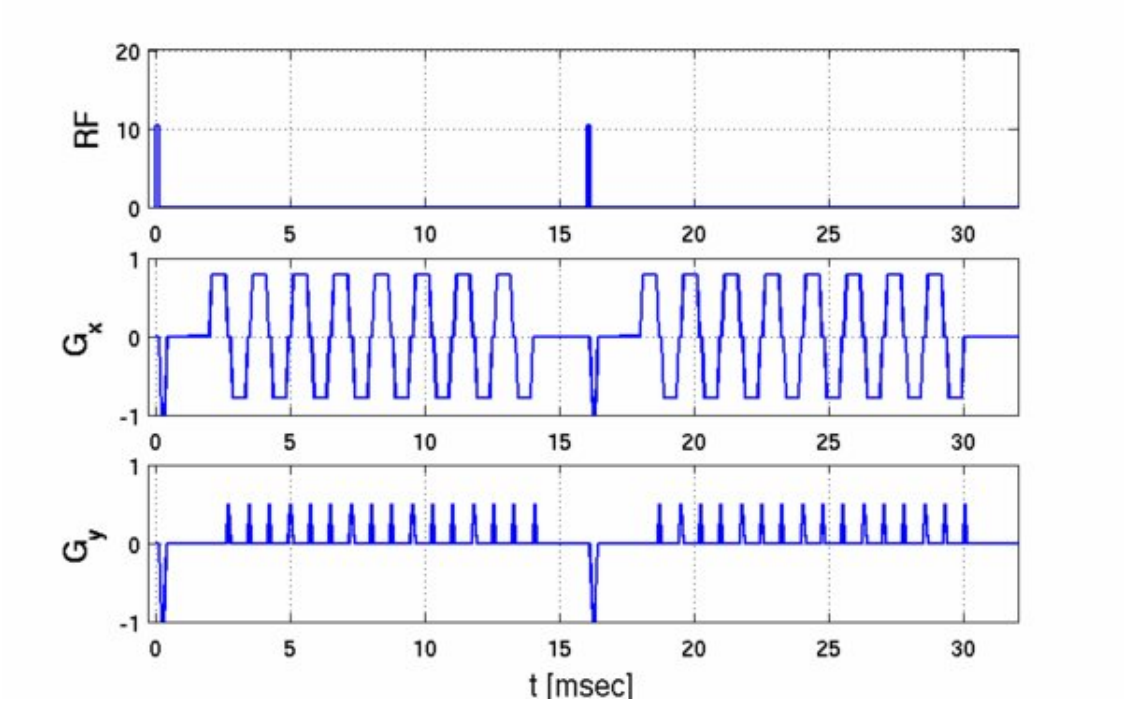


Figure 3: the RF, the read and the phase signals[9]

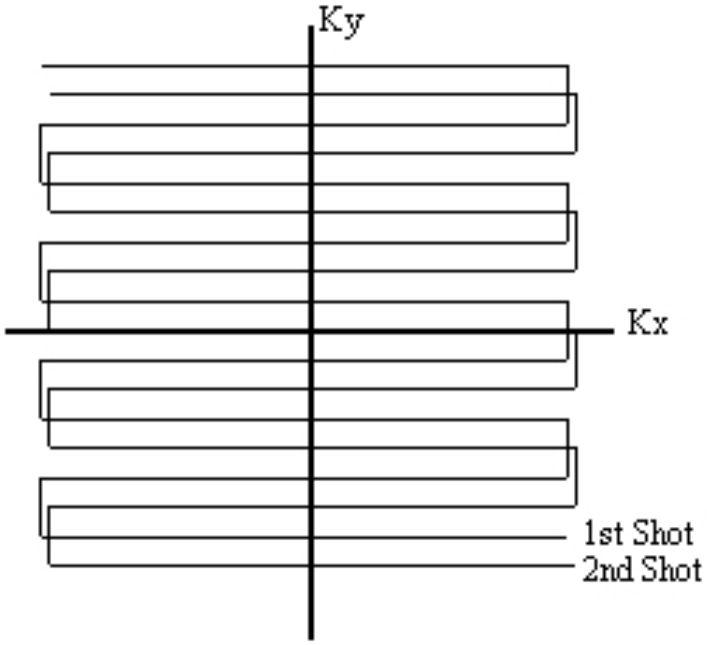


Figure 4: The two shot interleaved EPI[10]

## 2.2 Preprocessing the brain images

After MRI measures the brain data will be preprocessed. The preprocessing steps are made to remove artifacts from the brain images and to make the subjects' brains comparable in the future statistical analysis. The preprosesecing steps convert the raw MRI data into images that look like brains. These steps, after the k-space data is reconstructed into a 3D-image, are shortly explained in this section.[7]

### 2.2.1 Motion correction

People should stay still in MRI scanner when brain activity is measured. However when the measure takes several minutes muscles get tired and little motion is mandatory. These moves affect the pictures so that after a movement the same part of the brain appears in different voxel as it was before the movement. When processes in a certain area of the brain, for example in a voxel, are explored for the whole series of the measurements the accidental motion moves the monitored part to a different voxel. This can be prevented by the motion correction and it is very important for structural and functional brain image analysis. The motion also creates artifact to data which can be separated by the motion correction from the real activation.[8]

In the forthcoming statistical analysis it is assumed that the location of a given voxel within the brain does not change over time. This is why the motion must be estimated and corrected. Normally with fMRI a reference image is selected from within the series and other images are registered to that selected fixed image.[8]

### 2.2.2 Slice time correction

A fMRI picture is taken during the time of TR. The picture is collected one slice at the time meaning that the first slice will be taken almost one TR before the last slice. When TR is 2 seconds the gap is big between the first and the last slice. Here the slice time correction can be used to correct the slightly different time taken slices to respond to the wanted time. In 2 seconds a lot of things can happen in the brain so it is important to remember that different slices do not exactly correspond to each other. Also the future analysis assumes that the slices are collected at the same time. Slices can be taken in regular up (1, 2, 3, . . . , n), regular down(n, n-1, . . . , 1) or interleaved order (2, 4, 6, . . . , n, 1, 3 ,5 , n-1). It is necessary to know in which order the slices of the image where taken to succeed in the slice time correction.

### 2.2.3 Brain extraction

Functional MR images often contain little and high resolution MR images contain a lot of non-brain tissue. There are fat, the skull, the muscles, the eyeballs etc. besides the brain. The idea of the brain extraction is to remove these non-brain tissues. The removal is important for the registration and the future analysis to be successful. The brain extraction will be done after the motion and the slice time correction.[11]

There have been three main methods for the brain extraction. To do it manually that can be done fairly accurately. However it's time consuming to do the extraction manually and sufficient training is required. Another way is thresholding with the morphology[12] where an intensity thresholding is applied. This is usually a semi-automated method where the user normally helps to choose the thresholds. The aim is to separate image into the dark parts (scull, background), the light parts (eye balls etc.) and the less light part (brain tissue). The brain should be found by finding the largest unbroken cluster which is not the background. The largest cluster almost always still contains some non-brain tissue via a thin strand of the bright voxels. These areas are disconnected with the morphological filtering where the links are eroded. The largest cluster is then chosen and extended back to same extent as before erosion.[11]

The third way is to use the deformable surface models where a mesh is fitted to the brain surface in the image. There is normally a constraint that forces some smoothness to the surface. The model is also fitted to a correct part of the image and the surface is iteratively deformed from the starting point until the optimal solution is found. This is probably the easiest of these three methods to automate.[11]

### 2.2.4 Spatial smoothing

The spatial smoothing will improve signal to noise ratio of an image. At the same time it reduces resolution. The smoothing is normally done in an area between 5-15 mm. If small areas are explored a smaller smoothing should be selected and when larger areas are studied a larger smoothing can be applied. The problem in the smoothing is that voxels near to the area of interest might affect the value too much and change the real effect.[10]

Table 1: 9 point filter

| | | |
|---|---|---|
| 1 | 2 | 1 |
| 2 | 4 | 2 |
| 1 | 2 | 1 |

The idea of the spatial smoothing can be explained by using a simple 2-d 9 point filter (table(1)) where the target pixel in the middle has the strongest effect to the coming value and the surrounding pixels affect less. The value of the pixel is calculated as a weighted sum of the pixels. If $S(x, y)$ is the intensity at a position $(x, y)$ the smoothed intensity is

$$\begin{aligned} S'(x,y) &= \frac{S(x,y)}{4} \\ &+ \frac{S(x-1,y)+S(x+1,y)+S(x,y-1)+S(x,y+1)}{8} \end{aligned}$$

$$+ \quad \frac{S(x-1,y-1)+S(x+1,y+1)}{16}$$
$$+ \quad \frac{S(x-1,y+1)+S(x+1,y-1)}{16} \tag{14}$$

Normally some type of Gaussian kernel is applied in stead of the 9 point filter. For example a three dimensional Gaussian kernel might be applied

$$f(x,y,z) = exp(-(\frac{x^2}{2s_x^2} + \frac{y^2}{2s_y^2} + \frac{z^2}{2s_z^2})) \tag{15}$$

where $s_x$, $s_y$ and $s_z$ are the standard deviations.[10]

### 2.2.5 Temporal filtering

The temporal filtering will improve signal to noise ratio. It will remove long frequencies or low frequencies from the data often caused by the scanner or other parts of the body. Each voxel's time series is smoothed separately in the Fourier domain. The filtering must be done with care so that the signal of interest will not be lost. For example there might be low drifts caused by the brain too.

### 2.2.6 Registration

Human brains differ in size and shape. The corresponding parts of each brain might locate in different voxels of the scanned images. To make the brains comparable to each other and to define a spatial relationship a registration to a standard brain is used. This means transforming the brain to correspond a common template brain.[7]

The linear and the non-linear transformation are two common classes of the transformation. In the linear transformation there are 12 or less degrees of freedom (DOF) and in the non-linear transformation there can be millions of DOF. In linear transformation there are three translations, three rotations, three scaling and three skew parameters one for each axel. Commonly the rigid body (6-DOF) including translation and rotation, the similarity (7-DOF) including translation, rotation and a global scaling or the affine transformation (12-DOF) including all parameters are used. Only the translation and the rotation should be necessary for a good registration but in practice DOF is often increased to 12 or even the non-linear transformation is used to get a better registration.[7]

The Talairach space from atlas of Talairach and Tournoux 1988 and the Montreal Neurological Institute (MNI) space are two commonly used spaces where the images are registered. The Talairach space is based on a single brain of a 60 years old woman. The MNI space is a combination of MRI scans on normal controls.

#### Registration for fMRI

The registration will be performed after the other preprocessing stages discussed earlier are done. Also non-brain structures from a structural image must be removed. Then there will be three registration stages to execute. At first the functional image

is registered to the subject's structural image then the structural image is registered to the template image. Finally these two transforms are combined. This process will be performed to every measurement so that they will correspond to each other.[7]

### 2.2.7 Removal of artifacts

When brain activity is recorded with fMRI a problem with low signal to noise ratio is often encountered. In addition to the head motion there are other things causing artificial activation. Artifacts can be caused by the scanner, heart beat or breathing. Many physiological components are of higher frequencies than TR and are aliased within fMRI signal[13]. These are therefore hard to remove using filtering. These components can be found by the independent component analysis that maximizes independence. As the independent artifacts are found they can be removed from the original data to make future analysis better. Some methods for removing these artifacts have been developed by Thomas et al.[14],and Kochiyama et al.[15], Perlbarg et al.[16]and Tohka et al.[17]

## 2.3 Independent component analysis

The independent component analysis (ICA) is a signal processing method which can separate original signals from their mixed signals. When two people are speaking at the same time they produce two voice signals $s_1(t)$ and $s_2(t)$. If there are two microphones recording these voice signals two mixtures will be got of them

$$x_1(t) = a_{11}s_1 + a_{12}s_2 \tag{16}$$

$$x_2(t) = a_{21}s_1 + a_{22}s_2 \tag{17}$$

where $a_{11}$, $a_{12}$, $a_{21}$ and $a_{22}$ are parameters defining the attenuation of the original voice signals. ICA allows the estimation of $a_{ij}$ based on the information of their independence. As $a_{ij}$ is known the original signals can be separated from the mixed signals.[18]

Originally ICA was used for problems like the previous one or closely related to it known as the cocktail-party problems. Later ICA has been found useful for brain research. ICA is a powerful method for unmixing linear mixtures of unknown independent sources[19]. It is nowadays used to separate signals in electroencephalogram (EGG) and fMRI studies.[18]

### 2.3.1 Basic principles of ICA

Instead of sums as in the equations 16 and 17 the vector-matrix notation will be used. Let $x$ be a random vector whose elements are the observed values $x_1, x_2, \ldots, x_m$, and $s$ is a random vector whose elements are the sources $s_1, s_2, \ldots, s_n$. A is a square mixing matrix with elements $a_{ij}$. The mixing model can be written

$$x = \mathbf{A}s \tag{18}$$

where $x$ is a linear combination of different sources.[18]

ICA is closely related to the blind source separation (BSS). The idea is to estimate the mixing matrix A and calculate its inverse W so that the independent source values $s_n$

$$s = \mathbf{W}x \tag{19}$$

can be determined. The order of the independent components can not be determined. The sources can be in different order in two tests with the same observed values. The resulting sources might also be multiplied by -1. However these do not matter in most applications. All independent components must be nongaussian except one because the mixing matrix A is not identifiable for Gaussian independent components.[18]

To find the independent components gaussianity is minimized. A nongaussian component gives a good approximation for an IC because the sum of two independent variables $s_n$ is always more Gaussian than the original variables. There are many ways to minimize the gaussianity. Hyvärinen and Oja[18] write about kurtosis, negentropy, minimization of the mutual information and maximum likelihood estimation as ways to minimize the gaussianity.[18]

Normally there are two preprocessing steps in ICA centering and whitening. In the centering $x$ is made zero-mean. In the whitening vector $x$ is transformed linearly so that its components are uncorrelated and their variance equal unity.[18]

### 2.3.2 Probabilistic ICA model

There are few problems in the ICA model. The mixing matrix $A$ is assumed to be square and there is no noise included to the model. These problems have been solved by probabilistic ICA (PICA)[20]. PICA allows a nonsquare mixing process and assumes that data has some Gaussian noise

$$x = \mathbf{A}s + \mu. \tag{20}$$

The mixing matrix will be estimated from the data. PICA is specially optimized for fMRI data analysis. The idea is to decompose the data into independent maps which describe different activation patterns. ICA also separates artifacts from the real data. ICA does not need a model for signal separation and that's why it is useful in brain research.[20]

In PICA there are different stages. At the first stages a signal-noise subspace is estimated. This is done by employing probabilistic principal component analysis (PCA) [21]. Then the independent components are estimated from the subspace by maximizing the non-gaussianity using a fixed-point iteration scheme[18]. Finally the statistical significance of the components will be assessed. The ICA estimates are transformed to Z-scores based on the estimated standard error of the residual noise.[20]

In the model the noise covariance matrix $\Sigma_i$ is assumed to be known. Then the data can be whitened with the respect of the noise covariance. In PICA it is assumed that noise and signal are uncorrelated and

$$R_x - \sigma^2 I = AA^t \tag{21}$$

where $R_x = \langle x_i x_i^t \rangle$ is the covariance matrix of the observation. Let $X$ be the $p \times N$ matrix of the voxel-wise prewhitened data vectors where $p$ is the number of observations. The singular value decomposition of $X$ is $X = U(N\Lambda)^{\frac{1}{2}}Q^t$. If the number of sources $q$ is known we can estimate

$$\hat{A}_{ML} = U_q(\Lambda_q - \sigma^2 Iq)^{\frac{1}{2}}Q^t \tag{22}$$

where $U_q$ and $\Lambda_q$ contain the first eigenvectors and eigenvalues of $U$ and $\Lambda$ and where $Q$ denotes the $q \times q$ orthogonal rotation matrix.[20]

After whitening data with respect to the noise covariance and projecting the temporally whitened observations onto the space spanned by the $q$ eigenvectors of $R_x$ with the largest eigenvalues, the estimation of the mixing matrix $A$ reduces to identifying the square matrix $Q$. Then generalized least-squares is used for ML estimates

$$\hat{s}_{ML} = (\hat{A}^t\hat{A})^{-1}\hat{A}^t x \tag{23}$$

$$\hat{\sigma}^2_{ML} = \frac{1}{p-q}\sum_{p}^{l=q+1} \lambda_l \tag{24}$$

By iterating the estimates $\hat{A}$ and $\hat{s}$ and re-estimating the noise covariance from the residuals $\hat{\eta}$ the model can be solved in the case of full noise covariance.[20]

The source distribution is assumed to be Gaussian and probabilistic PCA[21] can be used to estimate the number of sources $q$. To complete the estimation the orthogonal rotation matrix $Q$ is optimized in the whitened space. Here a fixed point algorithm by Hyvärinen and Oja[18] is used that uses negentropy in order to estimate the non-Gaussian sources. The sources are catered by projecting the data onto the individual rows of $Q$. The $r$'th source is estimated

$$\hat{s}_r = v_r^t(\tilde{x}) \tag{25}$$

The source estimates are optimized by a contrast function

$$J(s_r) \propto \langle F(\hat{s}_r)\rangle - \langle F(\nu)\rangle \tag{26}$$

where $\nu$ is a Gaussian variable of zero mean and unit variance and $F$ is a non-quadratic function[22]. The vector $v_r^t$ is optimized to maximize $J(s_r)$ using the approximate Newton method.[20][18]

Finally individual ICA-maps $s_r$ are converted into Z-statistic by dividing IC-maps by the estimate of the voxel-wise noise standard deviation. Gaussian mixture models are fitted to these Z-scores to find out the significance of each voxel. The distribution of the spatial intensity values of the rth Z-map is modeled by K mixtures of 1-dimensional Gaussian distributions[23]

$$p(z_r \mid \theta_K) = \sum_{l=1}^{K} \pi_{r,l} N_{z_r}[\mu_{r,l}, \sigma^2_{r,l}] \tag{27}$$

where $\theta_K = [\pi_K, \mu_K, \sigma_K]$ and $\pi_K$,$\mu_K$,$\sigma_K$ are the vectors of the K mixture coefficients, means and variances. This model is fitted using the expectation-maximization algorithm[24] and an approximation to the Bayesian model evidence is used to find the correct number of mixtures.

It is asumed that the first term in the mixture models the background noise. The posterior probability for activation is calculated by dividing the other mixtures by the whole distribution[25]

$$Pr(activation \mid z_{r,i}) = \frac{\sum_{l=2}^{K} \hat{\pi}_{r,l} N_{z_r}[\hat{\mu}_{r,l}, \hat{\sigma}^2_{r,l}]}{p(z_r \mid \hat{\theta}_K)}. \tag{28}$$

Final PICA-components are formed using a certain significance level. The whole PICA process is illustrated in figure(5).[20]

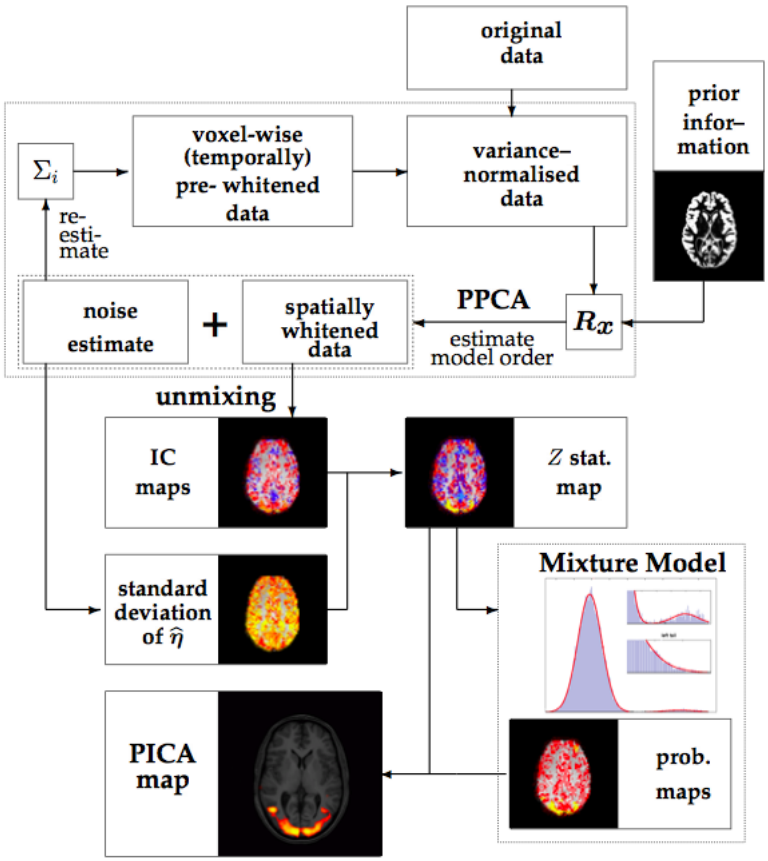


Figure 5: pica[20]

### 2.3.3 Group analysis

The brain activity between different individuals differs from each other during the measurement. However there might be some common patterns between all of the individuals or at least maturity of them. To compare similarities between the subjects a group analysis can be used. One method to compare similarities, where a stimulus is consistent between subjects, is the multi-session tensor-ICA which is derived from the Parrallel Factor Analysis[26].[27]

In tensor-ICA data is represented in 3D-array

$$x_{ijk} = \sum_{r}^{R} a_{ir} b_{jr} c_{kr} + \epsilon_{ijk} \tag{29}$$

where $i = 1, \ldots, I; j = 1, \ldots, J; k = 1, \ldots, K$ and the dimensions are time, space and the subjects. This is decomposed into three factor matrices A, B and C, time and the components, space and the components and the subjects and the components. The problem can be solved using the Alternating Least Squares (ALS) by iterating least squares solution for

$$X_{i..} = B\Lambda(a_i)C^t + E_{i..} \qquad i = 1, \ldots, I \tag{30}$$

$$X_{.j.} = C\Lambda(b_j)A^t + E_{.j.} \qquad j = 1, \ldots, J \tag{31}$$

$$X_{i..} = A\Lambda(c_i)B^t + E_{..k} \qquad k = 1, \ldots, K \tag{32}$$

where $\Lambda(a_i)$ is the $R \times R$ diagonal matrix where the diagonal elements are taken from the elements in row $i$ of $A$.[27]

These can be alternatively expressed as a matrix products. For example equation (32) can be expressed

$$X_{IK \times J} = (C| \oplus |A)B^t + \tilde{E}. \tag{33}$$

Tensor-ICA directly estimates separate modes in the three domains. It does not treat all modes of the variation as equal. Tensor-ICA puts stronger statistical constraints on the spatial domain where a lot of data is available. The model is formulated so that it includes the assumption of the maximally non-gaussian distribution of the estimated spatial maps. The algorithm has two stages. Estimate $B$ from $X$ by estimating $M$ as the mixing matrix using PICA

$$X_{IK \times J} = MB^t + \tilde{E}. \tag{34}$$

and decompose the estimated mixing matrix $M$ such that

$$M = (C| \oplus |A) + \tilde{E}_2. \tag{35}$$

This is continued until convergence.[27]

## 2.4 Intersubject correlation

The intersubject correlation is a model-free technique where an activation of the reference subject is used to predict an activation of the other subjects. The prediction is done by calculating the correlation coefficient between the time courses of the two subjects. When different subjects brain activity is compared with the intersubject correlation during a natural viewing there does not have to be any prior design matrix or assumptions of the functional responses. The parametric mapping is based on the similarity in the blood oxygenation level dependent signal between the subjects[28]. Hasson et al.[1], Golland et al.[29], Jääskeläinen et al.[3] and Kauppi et al.[28] have used the intersubject correlation analysis to analyze fMR brain images taken during watching movies.[1]

### 2.4.1 Correlation

Correlation measures the degree of statistical relationship between random variables or observed data values. A familiar measure of the dependence between two variables is the Pearson's correlation coefficient

$$r = \frac{\sum_{i=1}^{n}[(x_i - \bar{x})(y_i - \bar{y})]}{\sqrt{\sum_{i=1}^{n}(x_i - \bar{x})^2 \sum_{i=1}^{n}(y_i - \bar{y})^2}} \tag{36}$$

where $x_1, x_2, \ldots, x_n$ and $y_1, y_2, \ldots, y_n$ are the random variables and $\bar{x}$ and $\bar{y}$ are the means of the random variables.

The Pearson's correlation coefficient will give values between -1 and 1 reflecting the linear relationship between the variables. The closer the value is to -1 or 1 the stronger the dependence as 0 tells that the variables are independent. Positive values mean a positive dependence and negative values reflect a negative dependence.

### 2.4.2 Intersubject Correlation Analysis

The intersubject correlation analysis is developed for processing natural stimuli in group fMRI data. The time series of the subjects' brain activity are compared voxel-by-voxel basis with a chosen similarity criteria. Similarities are calculated to the whole brain. In the intersubject correlation analysis tool[28] the fMRI time series are divided to frequency subbands and the same calculations are repeated for them. The calculations are first done between every subject pair and from those a single index is calculated which describes the total similarity.[28]

A wavelet filter bank is constructed using the stationary wavelet transform. The J-scale wavelet filter bank is built using the Daubechies 2 quadrature mirror function pair in order to perform the frequency analysis. This way J+1 frequency subbands will be obtained.[28]

The correlation is first calculated over every brain voxel between every pair

$$r_{ij} = \frac{\sum_{n=1}^{N}[(s_i[n] - \bar{s_i})(s_j[n] - \bar{s_j})]}{\sqrt{\sum_{n=1}^{N}(s_i[n] - \bar{s_i})^2 \sum_{n=1}^{N}(s_j[n] - \bar{s_j})^2}} \tag{37}$$

where $N$ is a number of samples, $s_i$ and $s_j$ are the time series of $i$'th and $j$'th subject and $\bar{s_i}$ and $\bar{s_j}$ are the corresponding means. Then the pairwise correlations are averaged

$$\bar{r} = \frac{1}{(l^2 - l)/2} \sum_{i=1}^{l} \sum_{j=2, j>i}^{l} r_{ij} \tag{38}$$

to get a sigle index that gives group level information. The number of subjects is denoted by $l$.[28]

The calculations are also done in shorter time frames in addition to the whole data. The data is windowed to equally long time series each beginning a certain time step after the previous one. The same time points can appear in many consecutive windows if the time step is shorter than the size of the window. A time series from the number of the correlating voxels in the windows can be constructed. The voxels can also be selected from a brain region of interest and only it can be explored. The windowing gives more accurate information of the synchronizations at the different time points. This can be used in finding the stimuli causing the dependencies in the brain responses. It is easier to find the stimuli causing the correlations when overlapping windows are used.[28]

A voxel-wise permutation test similar to Wilson et al.[30] was performed to test the signifigance of the results. Each subject's time series were randomly circularly shifted to calculate $r$ statistic. The resulting p-values were corrected using False Discovery Rate with independence or positive dependence assumption.[28]

### 2.4.3 False Discovery Rate

Brain images contain over 100,000 voxels. When thresholding 100,000 voxels at $\alpha = 5\%$ threshold, 5000 false positives would be expected in null data and is therefore inappropriate. The false positives must be controlled over all tests. The familywise error rate (FWE) has been the standard measure of the Type I errors in multiple testing. It is the probability of any false positives.[31]

Benjamini and Hochberg[32] introduced Bonferroni related method the false discovery rate (FDR) control which has a greater control than FWE. The Bonferroni inequality is a truncation of Boole's formula[33]. It gives

$$p_i = \frac{\alpha_0}{V} \tag{39}$$

where V is the number of null hypothesis, $\alpha_0$ is the treshold and $p_i$ p-value of the test i. However it did make no assumption on dependence between tests which near voxels in fMRI data have. FDR was proven to be valid under independence by Benjamini and Hochberg. Later Benjamini and Yekutieli[34] showed that the FDR method is valid also under dependence. FDR with the independence or positive dependence assumption has the form

$$p_i \leq \frac{\alpha_0 * i}{V} \tag{40}$$

It is a step-up test which proceeds from the least to the most significant p-value. The first that satisfies the equation implies that all smaller p-values are significant.[31]

## 2.5 The previous studies of ICA and ISC

There have been many neuroimaging studies where a same fixed stimulus is presented for different humans whose brain activity is monitored at the same time. Pictures are presented or sounds are created to make stimuli for brain. The tests have been restricted and therefore the possibility for an individual variation has been low. Recently studies have moved towards a more natural environment. For example movies are presented where brains receive different stimuli continuously. Subjects can freely move their eyes and they might pay attention to different parts of the scene. Also connected plot and different characters create strong emotions. Bartels and Zeki[2] and Hasson et al.[1] used movies to create more naturalistic stimuli.

Hasson et. al. used intersubject correlation analysis where voxels' time courses of one brain were used to predict the activity in other brains. Also the reverse-correlation method was applied. It uses the brain activation to find the stimuli in the movie. The time points of the activation in a particular part of the brain where located. The movie was then examined from these same time points to find the stimuli that caused the activation in this particular region. They showed a 30 minute segment of the movie "The good, the bad and the ugly". The movie was assumed to give a much richer and complex stimulus than constrained visual stimuli in the laboratory.[1]

Hasson et. al. found out that the brains of the different individuals have a tendency to act the same way during free viewing of the movie. Significant inter-subject correlations were found in the well-known visual and auditory cortices and also in the high-order association areas. The reverse-correlation approach was used to study the time courses of the face related posterior fusiform gyros and the building related collateral sulcus. The highest peaks of both regions' time courses were compared to related frames of the movie. 15 of the 16 highest peaks in the fusiform gyros were associated with face images and 13 out of the 16 highest peaks of the collateral sulcus were associated with scene images. These brain regions maintained their selectivity under free viewing of the complex scenes.[1]

From regions that are typically not activated with these kind of stimuli Hasson et. al. studied areas where the intersubject correlation was significant. They found regions that could be related to action in the movie for example a cortical region located in the middle postcetral sulcus was connected to hand movements in the movie.[1]

Independent component analysis was first used for fMRI data by McKeown et al.[35]. Bartels and Zeki[2] showed a clip of the movie "Tomorrow never dies" to 8 subjects and monitored their brain activity during the movie. They used ICA to separate independent components from the data. They selected ICs whose most significant voxels corresponded anatomically and which had significant intersubject correlations. In almost every subject they found 10 ICs whose most significant voxels corresponded across subjects. Most of these components were anatomically

located in the visual processing areas and the auditory areas. They found that the functional organization of the brain during natural conditions was preserved, ICA detected voxels that belonged to different subdivisions and cortical subdivisions were separated to different ICs.[2]

Jääskeläinen et al.[3] studied emotions by viewing the movie Crash. fMRI was measured during a free viewing of the movie. They calculated the intersubject correlations which was high in many cortical and subcortical areas. Also many prefrontal cortical areas were significantly correlated. They did also an ICA analysis which expose ICs from the primary visual areas V1, V2 and V5 but they could not find clear events that caused those ICs. ICs that had a clear connection to the movie were related to auditory activity. Two ICs showed activation when there was speech in the movie. However these ICs did not show activation when there was music or non-speech sounds in the movie.[3]

Kauppi et al. divided the fMRI data from the movie Crash to subbands. A common value for the group intersubject correlation was calculated to the full band and every subband separately. Correlation was found in the auditory and the visual processing areas in high frequencies. Low frequencies showed correlation also in frontal part of the brain.[28]

### 2.5.1 Consistency and variability of ICA

Solution in ICA can slightly change each time the method is applied. A statistical study can be done to find how stable the method and different ICs are. This will reveal the importance of the resulting components. It also reveals how different components are divided in different analysis. Jarkko Ylipaavalniemi presents a method in his master's thesis which measures stability of the independent components[36]. He has used bootstrapping to measure variability of the independent components.

At first multiple ICAs are run. Then the resulting independent components are clustered spatially. From those clusters the spatial variability can be measured. Also the temporal changes between the spatially corresponding components can be seen.[36]

ICA is run multiple times and the results are concatenated together

$$A^{all} = [A^1 \mid A^2 \mid \ldots \mid A^n] \tag{41}$$

where each column of $A^{all}$ defines an independent component and matrix $A^n$ defines the mixing matrix of the $n$'th run. Before the estimates are clustered they are made zero mean and unit variance. The similarity of the normalized ICs is measured by calculating the correlation of each IC pair which forms a correlation matrix

$$C \propto A^T A. \tag{42}$$

In order to find significant similarities each element of the correlation matrix $C$ is thresholded with a value $k$

$$c_{ij} = \begin{cases} 1, & \text{if } |c_{ij}| > k \\ 0, & \text{if } |c_{ij}| < k \end{cases}$$

where all interesting correlations get the value one and others get the value zero forming a binary correlation matrix $\hat{C}$.[36]

The matrix shows the relation between adjacent estimates $a_i$ and $a_j$ which will be put to the same cluster. If $a_j$ is also related to $a_k$ but $a_k$ is not straight related to $a_i$ it is still recommended to put $a_i$ and $a_k$ to the same cluster. These longer paths can be found by raising the correlation matrix to a power

$$R = \hat{C}^d \tag{43}$$

where $d$ defines the longest acceptable path.[36]

The ICs are clustered with a method where all ICs that have $r_{ij} > 1$ are sorted in descending order according to $c_{ij}$. Then the list is gone through. If linked estimates $a_i$ and $a_j$ do not belong to a cluster a new cluster is created. If either of the components belongs to an existing cluster the other one is added there too. If both belong to an existing cluster nothing is done.[36]

There are also other ways to cluster ICs. One is explained here. The group ICA is first run with all subjects. Then N numbers of bootstraps are run with the same subjects. The resulting ICs from the original run are gone through from the first to the last and from all bootstrap runs corresponding components are found and put to the same cluster. If the best fitting bootstrap component is already occupied by another IC of the original run the second best component will be tried. This is continued until a free component is found. From the components in one cluster an IC estimate is calculated as weighted average of the components using correlation to the old estimate as a weight. In the first step the original run is used as the old estimate and later the previous estimate is applied.

The bootstrap runs are gone through in an ascending order and all components in a run will be tested in an ascending order. If a component fits better to another estimate and changing position of this component with the component belonging to the other cluster makes the model better the positions will be changed otherwise nothing is done. After a change the estimates are updated. When all runs are gone through the examination will move back to the first run. This will be continued until convergency.

# 3 Research material and methods

## 3.1 Subjects

Twelve subjects participated to the study. To make sure that the subjects did not have any obstacles for participating to fMRI study they filled a safety questionnaire. An approval to the study was obtained from the subjects. All subjects were Finnish because the audio track of the movie was in Finnish.

## 3.2 Experiment

A 23 minute clip from the beginning of the movie Tulitikkutehtaan tyttö was shown to the subjects. The subjects were instructed to watch the movie freely like in the studies of Hasson et al.[1] and Bartels and Zeki[2]. The brain activity of the subjects was measured with fMRI during the movie.

The subjects removed all metallic objects before the scanning and a metal detector was used to secure the subjects safety and to prevent noise signals in fMRI. The subjects lay in a MRI scanner. The movie was projected onto a translucent screen which was viewed through an angled mirror. The auditory track of the movie was presented through auditory tubes and earphones. Headsets were also worn to prevent the noise of the scanner. The subjects were instructed to stay still during the scanning in order to avoid motion artifacts.

Functional brain images were taken with a 3.0 T GE Signa Excite MRI scanner (GE Medical Systems, USA) using a quadrature 8-channel head coil in the AMI Center at the Helsinki University of Technology. A total of 689 volumes of EPI were scanned. There are 29 slices in an EPI sequence with the repetition time (TR) of 2000 ms and the echo time (TE) of 32 ms. Images were obtained in axial orientation (thickness 4 mm, between-slices gap 1 mm, in-plane resolution 3.4 mm x 3.4 mm, voxel matrix 64 x 64, flip angle 90°).

Also an anatomical T1-weighted inversion recovery spin-echo volume was acquired (TE 1.9 ms, TR 9 ms, flip angle 15°). The T1 image acquisition used the same slice prescription as did the functional image acquisition, except for a denser in-plane resolution (in-plane resolution 1 mm x 1 mm, matrix 256 x 256).

## 3.3 Data analysis

The fMRI data was first preprocessed. After preprocessing the intersubject correlation analysis and the independent component analysis were run. These processes are explained here.

### 3.3.1 Preprocessing

FSL[37] software was used for preprocessing the EPI images. First MCFLIRT was used to remove the effect of head motion. Then the non-brain structures were removed with BET. BET was run to the motion corrected images resulting a single image. The motion corrected images were then masked with this image. A 10 mm

spatial smoothing was applied and the data was high pass filtered with 100s cutoff. 600s high pass filter was used for bootstrapping data. In order to make comparison of the different brains possible images were registered to the MNI template image. This was done by first registering the images to their structural images using 6 DOF and then registering the resulting images to MNI152_T1_2mm_brain standard brain using 12 DOF. 15 images from the beginning of fMRI were removed for ICA and 40 images were removed for the ISC analysis.

The structural images were skull-stripped using a customized procedure involving genetic algorithm based voxel classification[38] and Brainsuite2[39] program was used for brain extraction of the resulting images. A brain mask was created in Brainsuite2 by Brain Surface Extractor. The mask was used to removed the skull from the original T1-image.

### 3.3.2 Intersubject correlation

Before the intersubject correlations were calculated few artifacts were removed from each subject's data. FMRIB's FSL MELODIC was used to decompose the independent components from each subject's data separately. The resulting components from the verticles caused probably by the scanner and physical components from the white matter and the brain stem were removed. The removal was done with FSL.

The intersubject correlations were calculated using the intersubject correlation analysis tool[28] created by Jukka-Pekka Kauppi. In the tool the activity in brain is localized spatially as in previous studies and also in time and frequency. The time series was divided in 1 minute 12 seconds long parts containing 36 samples and step size between the windows was 18 seconds. The data was divided in 5 frequency subbands. The frequency bands are presented in table(2). The thresholds with three p-values 0.05, 0.005 and 0.001 were calculated and FDR-corrected for the subbands of the whole data and the windowed data separately.

Table 2: The frequency bands after the decomposition where $s^0[n]$ is the full band and the others are the decomposed subbands.

| **Set of coefficients** | **Frequency band (Hz)** |
|---|---|
| $s^0[n]$ | full band |
| $s^1[n]$ | 0.13-0.25 |
| $s^2[n]$ | 0.07-0.13 |
| $s^3[n]$ | 0.04-0.07 |
| $s^4[n]$ | 0.02-0.04 |
| $s^5[n]$ | 0-0.02 |

The intersubject correlations are calculated for all possible elements that the time series and the subbands create. The resulting data can be visualized by graphical user interface guided MATLAB software package.

### 3.3.3 Independent component analysis

The activity in the brain is a sum of many simultaneous independent components from different stimuli. With ICA it is possible to find out different independent components without any prior knowledge of the data, in our case, the brain images. Some of these ICs should have a connection to stimuli caused by the movie. Different functional areas in the brain react differently to different stimuli and form their own independent components.

The idea is to find out which areas of the brain are active and what happens in the movie at the same time. The time series of the activation in a particular region of the brain is examined. It is studied if similar stimuli happen in the movie during all or most of the peaks in the time series.

The aim is to detect the stimulus related independent components that are common in many subjects. FMRIB's FSL MELODIC software is utilized to decompose the independent components from the preprocessed data. In MELODIC the multi-session Tensor-ICA is used which combines the data from subjects and does a group independent component analysis to find independet components that are common to all the subjects. The number of ICs is limited to 50.

ICA is first run normally with 12 subjects to get estimates for clustering and then 100 bootstraps of ICA for 12 subjects were run to examine the consistency of the independent components. The resulting ICs were clustered using two clustering methods discussed in chapter 2.5.1. In a single link method introduced by Ylipaavalniemi et al.[36] a threshold value $k = 0.65$ for correlations was used. The longest acceptable path length was $d = 8$. The values were selected so that 100 auditory components that were found in all the bootstraps were placed to the same cluster. In the second method the number of clusters was limited to 50 each containing 100 components. First the Tensor-ICA was run with all the subjects to get the estimates for the 50 clusters. Then ICs from the bootstrap runs were clustered according to the estimates. Then all clusters were gone through 10 times to find a better fit. After the fifth lap the model did not get significantly better any more.

The estimates for the ICs can be calculated from these clusters. Spatial and temporal variability between the components in a cluster is also measured. This gives an idea how often different ICs appear in this kind of study. Also the nature of the variability becomes clearer. Some IC might vary strongly spatially when other might have a strong temporal variability. Bootstrapping gives more information about the method and the resulting independent components for the further study.

After the bootstrapping the IC maps were examined to detect the active area and then it was studied for what kind of stimulus in the movie might cause activation in that particular area. The highest peaks of the component's time series were compared to equivalent scenes in the movie and common events or factors were searched. These shared factors will probably cause activation in the specific area of the brain.

# 4 Results

## 4.1 Intersubject correlation

The intersubject correlation analysis was run for a group of 12 subjects. Thresholds were calculated for the resulting correlations at three significance levels at p-values 0.05, 0.005 and 0.001 for all bands of the whole data and the windowed data separately. The thresholds were FDR-corrected with independence or positive dependence assumption. To locate group intersubject correlation (GISC) in brain regions the Harvard Oxford probabilistic atlas with 50% threshold was used. This decreases errors caused of the anatomical variation. The neurological orientation is used in all brain images.

### 4.1.1 Whole data

In the full band major part of the voxels were active when results were thresholded at $p < 0.05$. At $p < 0.005$ there were still significant correlation in most parts of the brain. At $p < 0.001$ the most significant voxels had the superior and anterior part of the lateral occipital cortex and the precuneous cortex. Many smaller regions had most of their voxels significant. The highest correlations were found in the auditory and the the visual processing areas which correspond previous studies. Also high correlations were found in the parietal areas. The correlations at $p < 0.001$ are shown in figure(6). The correlations are scaled from 0 to 0.5. Black correspond the small correlations and yellow the big ones.

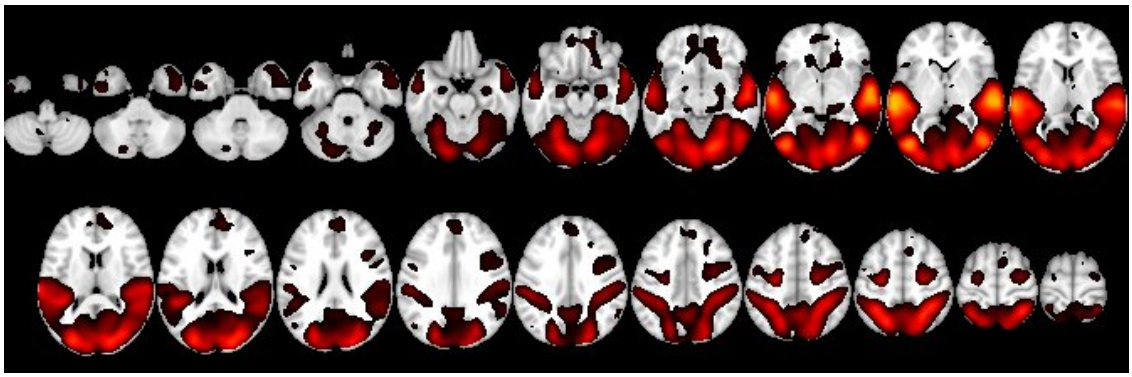

Figure 6: The intersubject correlations in the full band thresholded at $p < 0.001$. The correlations are scaled from 0 to 0.5. Black correspond the small correlations and yellow the big ones.

No significant correlations were found in the band 0.13-0.25 Hz at $p < 0.005$. Some significant correlations could be seen at $p < 0.05$ in the auditory and the visual processing areas. In the frequency band 0.07-0.13 Hz GISC was located in the visual and the auditory areas at $p < 0.001$ shown in figure(7). The occipital pole had the most active voxels. Also the posterior division of the superior temporal gyrus, the lingual gyrus, the lateral occipital cortex and the occipital fusiform cyrus

had many voxels that correlated at $p < 0.001$. Highest correlations were found in the auditory processing areas and the visual proseccing areas. Also the parietal areas showed some cor relation. At $p < 0.005$ significant part of the visual and the auditory cortices expanded and the parietal areas showed more correlation.

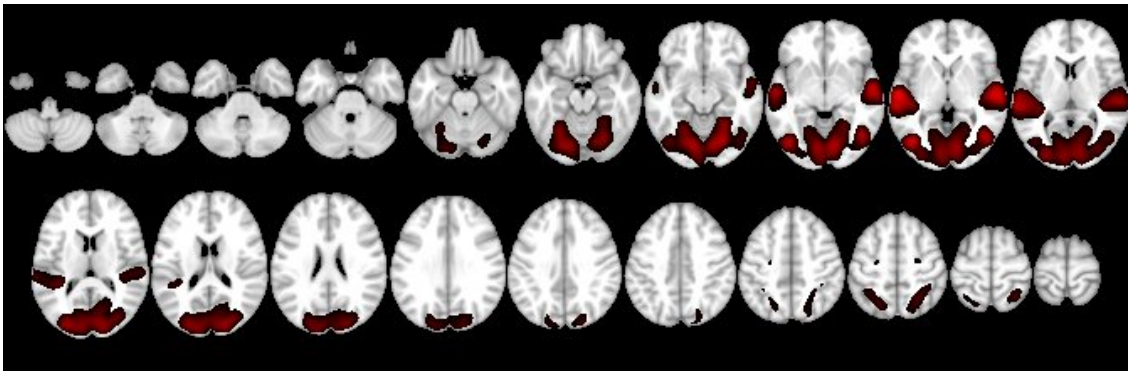

Figure 7: The intersubject correlations in the band 0.07-0.13 Hz thresholded at $p < 0.001$. The correlations are scaled from 0 to 0.5. Black correspond the small correlations and yellow the big ones.

With the frequency band 0.04-0.07 Hz GISC was found in the same areas as with the higher band. The occipital pole, both the superior and inferior division of the lateral occipital cortex and the lingual gyrus had most of the active voxels. The number of significant voxels in the occipital areas was much larger than in the higher frequencies. Also the motor cortex, the precentral gyrus and the anterior division of the supramarginal gyrus showed activation at p-value 0.001. The correlating areas are shown in figure(8) In practice the same areas were active at $p < 0.005$.

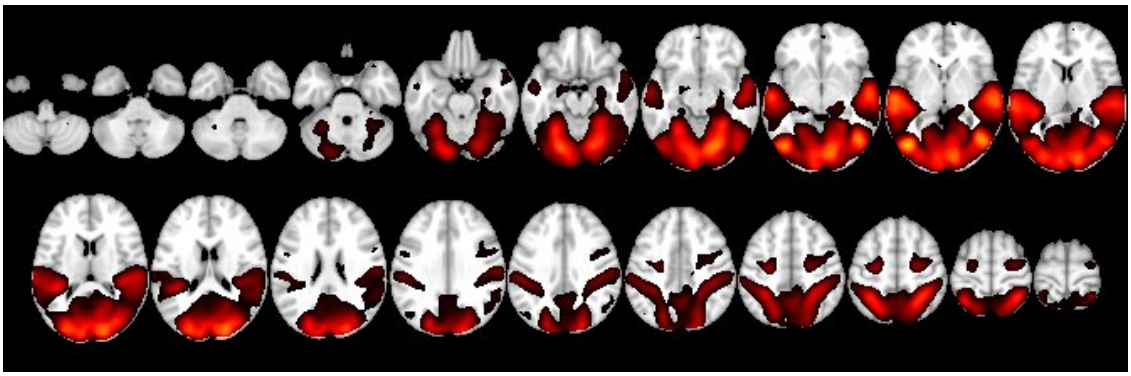

Figure 8: The intersubject correlations in the band 0.04-0.07 Hz thresholded at $p < 0.001$. The correlations are scaled from 0 to 0.5. Black correspond the small correlations and yellow the big ones.

The superior division of the lateral occipital cortex showed the most active voxels with the frequency band 0.02-0.04 Hz. The precuneous cortex had also many

significant voxels which was a clear increase from the band 0.04-0.07 Hz. GISC was widely spread on the occipital, the auditory and the motor areas. The first time significant correlation was found in the frontal cortex was with the frequency band 0.02-0.04 Hz. The amygdalas and the ventricles showed also some GISC at $p < 0.001$. Correlation in the ventricles indicates that some noise could not be removed in preprocessing causing correlations in low frequencies. Correlations at $p < 0.001$ are shown in figure(9). A large number of brain voxels showed correlation at $p < 0.005$. The highest correlations were found in voxel of the visual processing areas. Also the auditory processing areas reached to almost equal correlations.

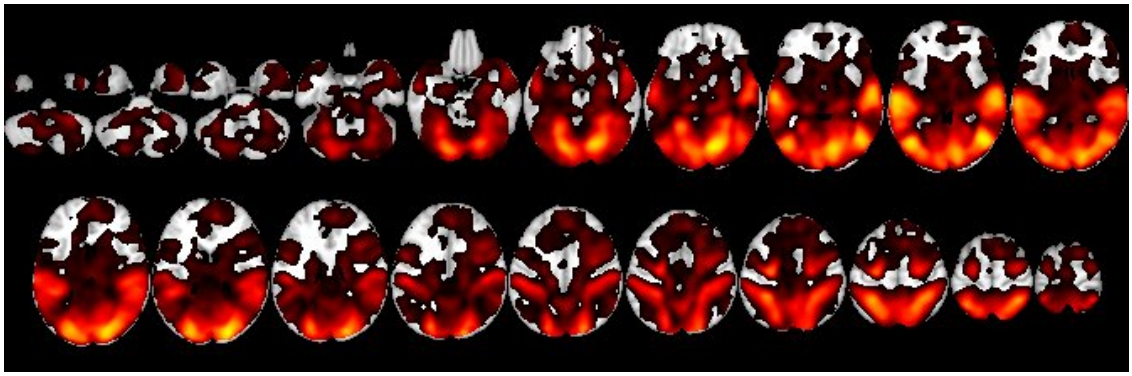

Figure 9: The intersubject correlations in the band 0.02-0.04 Hz thresholded at $p < 0.001$. The correlations are scaled from 0 to 0.5. Black correspond the small correlations and yellow the big ones.

In frequency band 0-0.02 Hz almost the whole brain showed GISC at the significance level $p < 0.001$ shown in figure(10). The highest correlations were located in the auditory processing areas. Correlation in the ventricles refers to low frequency artifact. The highest correlations appeared in the auditory processing areas. Clear decrease in correlation compared to the higher frequencies was found in the visual processing areas showing dominance of the high frequencies in visual processing. Respectively activation in frontal parts of the brain was found only in low frequencies.

For the 23min long movie along with accurate measurements the threshold values presented in table(3) are low at $p < 0.05$. Significant correlation is found all around the brain in low frequencies. Really clear areas of correlation can still be seen at more significant values $p < 0.005$ and $p < 0.001$ in all bands expect the band 0.13-0.25 Hz. GISC has found really reliable correlations in many regions for the whole movie.

### 4.1.2 Windowed data

As length of the data is reduced by windowing the movie to shorter clips, the threshold levels increase at the same three significance levels. The p-values and the corresponding threshold values are displayed in table(4) for the full band.

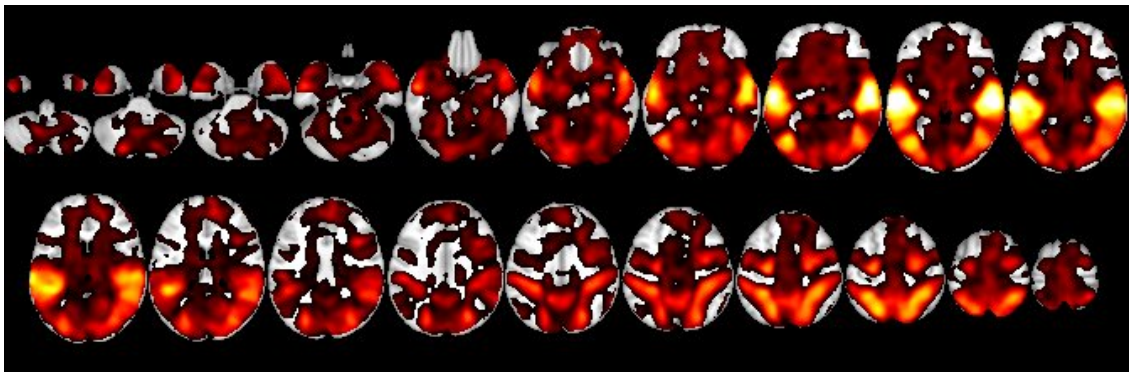

Figure 10: The intersubject correlations in the band 0-0.02 Hz thresholded at $p < 0.001$. The correlations are scaled from 0 to 0.5. Black correspond the small correlations and yellow the big ones.

Table 3: The frequency bands and the threshold values for correlations at the different FDR corrected significance levels for the whole data. No significant voxels were found in the band 0.13-0.25Hz.

| **Frequency band (Hz)** | $p < 0.05$ | $p < 0.005$ | $p < 0.001$ |
|---|---|---|---|
| full band | 0.02 | 0.05 | 0.07 |
| 0.13-0.25 | 0.05 | - | - |
| 0.07-0.13 | 0.03 | 0.06 | 0.08 |
| 0.04-0.07 | 0.02 | 0.05 | 0.07 |
| 0.02-0.04 | 0.02 | 0.05 | 0.06 |
| 0-0.02 | 0.02 | 0.05 | 0.06 |

Table 4: The threshold values for correlations in the full band at different FDR corrected significance levels for the windowed data.

| **Frequency band (Hz)** | $p < 0.05$ | $p < 0.005$ | $p < 0.001$ |
|---|---|---|---|
| full band | 0.20 | 0.49 | 0.52 |

Short window size in our case 1 minute 12 seconds raises the required threshold levels. By increasing the window size more significant correlations in various regions could be discovered but the accuracy when finding the stimuli causing the synchronizations from the movie suffers. The number of samples can not be dropped too low as the significance of the correlations decreases at the same time. There is 66 samples in a window which should reveal relevant correlations and make it possible to discover the stimuli from the movie. When studying the different subbands the band width should be taken into account when the window size is decided. As this has not been yet done the stimuli in the movie are only studied with the full band here.

In the full band at $p < 0.005$ only six regions had synchronization in several voxels of the posterior division of the superior temporal gyrus, the posterior division of the middle temporal gyros, the superior parietal lobule, the inferior division of the lateral occipital cortex, the occipital fusiform cortex and the lingual cyrus. These significant correlations were found only in a few windows. At significance level $p < 0.05$ correlations are found in many windows and in different brain regions.

### 4.1.3 Stimuli in the movie

The thresholded synchronizations in full band at $p < 0.05$ are presented as a color matrix in figure(12). A cell shows the number of the active voxels in a particular brain region in a window. Y-axis presents the brain regions and x-axis has the time points. On the right side k marks the maximum number of the correlating voxels and m stands for the total number of the voxels in the region. The colors are scaled

from zero to k. It is important to check the value of k because the regions are of different size and areas having more active voxels have more information. The same stimulus can be seen in six consecutive windows because they are overlapping. This can be seen in the figure(12) where many red cells come up in a row.

In the full band there are few time points where many voxels have significant correlation. At time points 7-9 there is singing in the movie which clearly activates the auditory areas. At time points 30-32, 39-41, 49, 53-59 and 67 there is speech in the movie. There also seems to be synchronization during these points in the auditory processing areas like the posterior division of the superior temporal gyrus. However music that is played in a bar between time points 15 and 22 does not create synchronization in any brain regions.

As speech seemed to cause correlation in the auditory processing regions no clear stimuli causing activation for other regions can be seen. One reason for this is the length of the window that is much longer than a simple stimulus. There are still clear scenes that cause correlation in certain voxels and brain regions. The visual processing areas have intersubject correlation in more windows than the other regions. There are also some parts that do not create any significant correlation in the brain regions. Here some of these scenes are gone through and pictures from the movie can be seen in figure(11). Time points of these pictures are marked in figure(12) as capital letters.

In the beginning of the movie there are only machines working creating no synchronizations. As a human appears in the movie at time point 2 (A) there seems to be some correlation in few brain regions, especially in the temporal part of the middle temporal gyrus. At time point 10 (C) a woman whose name is Iiris is writing her signature and receives her salary. The windows during this scene have much correlation in voxels of the inferior part of the lateral occipital cortex.

At time point 13 (D) the stepfather slaps Iiris in the face calling her a whore when she shows her parents a dress she has bought. Her mother tells to return the dress. There are many hand movements in this scene, taking the dress from a box, showing it and the slap. Correlation can be found in the superior parietal lobule, the temporal part of the middle temporal gyrus and the inferior part of the lateral occipital cortex caused probably by the motoric and the visual stimuli.

Between time points 16 to 25 there is a long part where no significant correlation can be seen. During these windows there is a scene in a bar where background music is played, faces are shown and Iiris and a man called Aarne are dancing as slow music is played (E). At time point 23 Aarne gets dressed and leaves a thousand Finnish marks to Iiris with whom he has spend the last night. During time points 24 to 25 Iiris wakes up and looks around Aarne's place. There is not action during these scenes and no clear stimuli can be seen which might be the reason that brain responses do not show much correlation.

Iiris writes down her phone number to a paper asking Aarne to call her at time point 26 (F) creating visual and motoric stimuli. At time point 27 she sorts match boxes with her hands (G) where the hand movement creates a motoric stimulus. During these scenes a great number of the correlating voxels can be seen in the superior part of the lateral occipital cortex, the occipital fusiform gyrus, the lingual

gyrus and the superior parietal lobule.

Between time points 30 to 33 there are many active regions mostly in the auditory and visual processing areas. In the movie Iiris waits for a call at 29 and then talks to Aarne at his place after he did not call at 31-33 where they agree for a date (H). The social intercourse between Iiris who has fallen in love and Aarne who does not really care might be the reason for this many correlating voxels.

There is another part where no synchronizations are found between points 34 and 38. In the movie people are just sitting at a café table (I) then Iiris and Aarne are walking to a car and finally they are eating in a restaurant. There is not much action during these scenes which might explain the lack of synchronization.

When Aarne recommends Iiris to leave and tells her that he has no feelings towards her at time points 39-41 (J) there is a rise in correlations in some regions especially in the intracalcarine cortex. The speech explains the correlation in the posterior part of the superior temporal gyrus.

After that there is a part where Iiris is lying down (K) and her mother is comforting her and smoking a cigarette after that. Their faces are shot during these scenes. These tranquil scenes create correlation in the occipital fusiform gyrus, the temporal occipital fusiform cortex, the lingual gyrus and the lateral occipital cortex. The faces shown are probably the main stimuli causing the brain responses.

A scene at time point 49 when Iiris hears from a doctor that she is pregnant creates correlation in many brain regions. Hearing of the pregnancy and zooming to her scared face (L) forms a really strong scene that stands up from the calm story telling of the movie. As there is speech in the scene correlation appears in the auditory processing areas like in the posterior part of the superior temporal gyrus. Synchronization can also be found in the visual processing areas. This scene creates correlation in many regions where there is not much correlation in the other part of the movie.

At time points 50-51 Iiris is working in the match factory putting match boxes in a machine (M). A lot of correlating voxels in different brain regions can be found during the scene. The superior and inferior part of the lateral occipital cortex, the occipital pole, the lingual gyrus and the precuneous cortex have the most correlating voxels. The Occipital fusiform gyrus, the temporal occipital fusiform cortex, the intracalcarine cortex, the anterior part of the supramarginal gyrus, the superior parietal lobule, the posterior part of the middle temporal gyrus and the posterior part of the superior temporal gyrus have also many correlating voxels. Also many other regions have their peak in the number of correlating voxels during this scene.

Between time points 54-59 Iiris is writing a letter. She speaks everything she writes. The camera is zoomed first to her head then at time point 56 the camera is zoomed out (N) and finally at time point 58 camera is zoomed to Iiris' hand. Here correlation is found in speech related the posterior part of the superior temporal gyrus and also in the posterior part of the middle temporal gyrus.

At time point 60 Iiris puts the letter into an envelope and licks edges of the envelop closing it. Between time points 61 to 64 Iiris receives a letter, opens it (O) and reads it. The camera is first zoomed to her hands and when reading the letter to her face creating correlation in the superior parietal lobule and the lateral occipital

cortex. At the end of the movie some correlation could be seen at time point 67 when Iiris' father talks to her.

As the brain regions having the most correlating voxels are studied the superior and inferior part of the lateral occipital cortex seem to have a lot of correlation in many windows. These areas are known to be related for the visual processing and as there are several visual stimuli in the movie these synchronizations are reasonable.

Another visual processing related region the occipital pole has many correlating voxels when Iiris is using the match machines in G and M and when many people are dancing and the band is playing in B. Correlation is also found when Iiris' stepfather slaps her at 14 and when she hears from her pregnancy at 50.

Voxels in the superior parietal lobule seems to correlate when stimuli related to hand movements are presented. The slap at 14 and Iiris ordering the match boxes at 28 and 51 and opening the letter at 62 all have a stimulus related to hand activity.


Figure 11: Examples of the movie scenes.

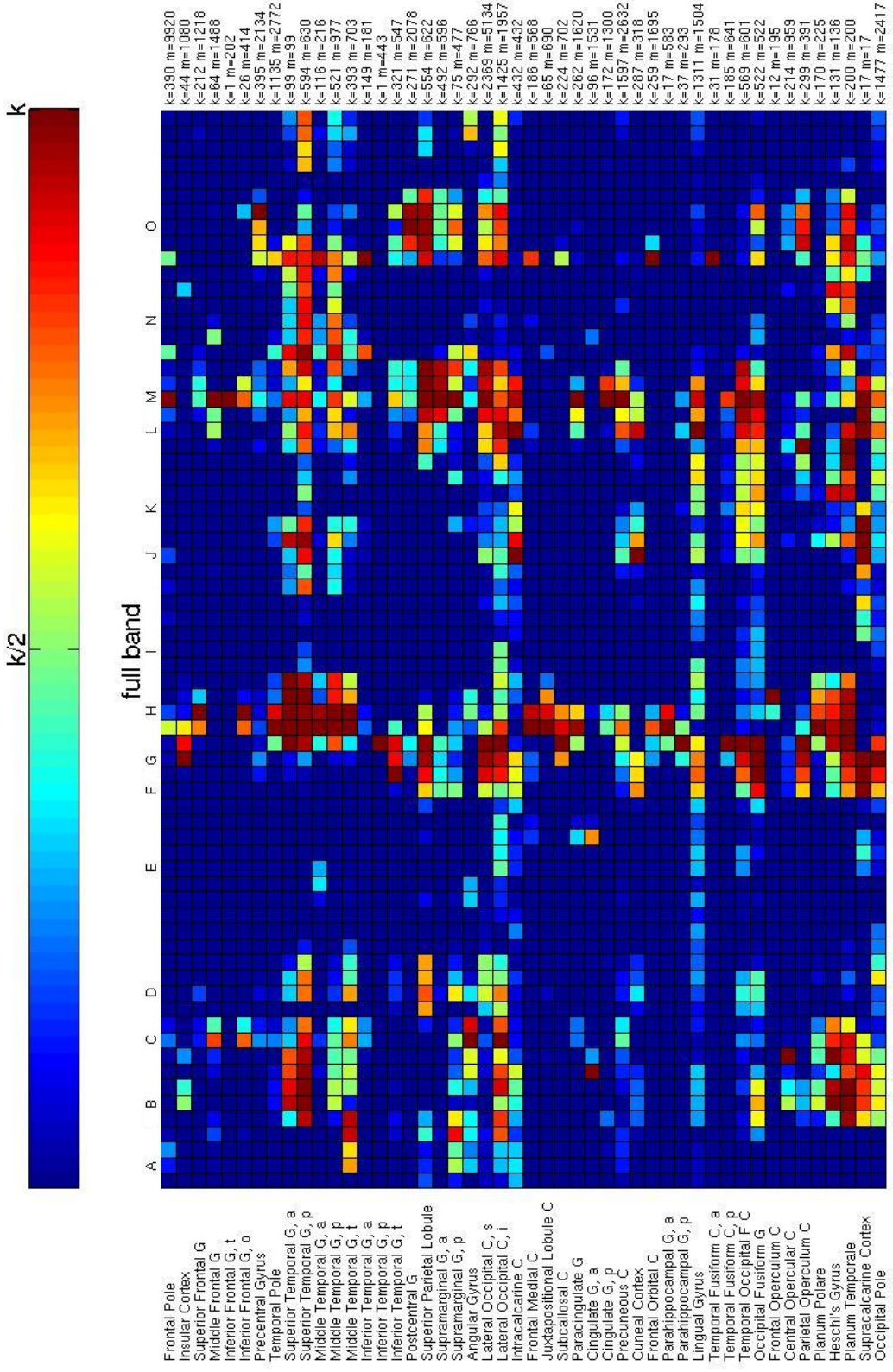


Figure 12: The intersubject correlations in the fullband for the windowed data thresholded at $p < 0.05$.

### 4.1.4 Comparison

The correlation calculated from the whole movie describes which brain regions have similar responses among the subjects over the whole data. For the whole movie the high correlations appear in the regions where stimuli are clear and continuous during the whole movie. Dividing the data in the different subbands allows studying the fast and the slow responses separately. The windowing allows the investigation of which kind of stimuli cause the responses. There are regions that might have high correlation only in a short part of the movie. By windowing, these regions can be found and the stimuli creating these responses can be searched from the movie more precisely.

The precision of the calculation decreases when the data is windowed. This can be seen in table(3) and table(4) where the threshold values are clearly higher with the windowed data. On the other hand many windows contain a clear area of the correlating voxels at $p < 0.005$ which are the most significant correlations and usually the most interesting too.

A window from the data does not answer accurately when the stimulus is presented in the movie. The stimulus causing the correlation can take place in any time point in the window and many stimuli causing brain responses in a same location of the brain might happen during a window length. This leaves us guessing when the stimulus has really happened. To locate the stimuli more accurately overlapping windows can be used. In our calculation the window size is 1 minute 12 seconds and step to next window is 18 seconds. Now the same stimulus appears in many windows helping in finding the stimulus causing the correlation.

## 4.2 Consistency of independent components

100 bootstrap runs of ICA were run to test the consistency of the resulting independent components. The components were clustered according to their spatial location. From the significant voxels of the components in a cluster contours were plotted to view their spatial variability and to find the most consistent components. Also the temporal variability of the components was tested. The neurological orientation is used in all brain images.

### 4.2.1 Clustering

The single-link clustering generated 697 clusters. Most of them were small clusters containing few components which were many times from a same bootstrap run. 53 clusters containing over 5 components existed. The most consistent component was the auditory component which was clear in every ICA. 9 clusters contained over 48 components, 16 clusters had 10 to 22 components and the rest had lower than 10 components. The 9 biggest clusters contained components from the auditory and the visual processing areas, one from the parietal area and one from the verticles.

The biggest clusters from the single-link method were also found with the second method where the number of clusters was limited to 50 and cluster size to 100 components. There were some noisy components put to almost every cluster because

every cluster had to have 100 components and if a well fitting component was not found from a bootstrap run a component that did not fit to any cluster was placed to that empty position. The new estimates were calculated as weighted sum so these noisy components did not affect to the new estimates.

In the single-link clustering threshold for correlation was ordered by the best correlating component. As a result with all the other clusters all components that might belong to a same cluster were not accepted to a same group but the actual cluster was divided to two or more separate clusters. Another problem with the single-link clustering is that two different clusters might be united to a cluster through a connecting component. This was the case with a component located to the middle temporal gyrus where there were three types of components. The first had activation on the right side of the brain, the second had activation on the left side and the third had both sides activated connecting these two clusters as one. This cluster was divided in two different clusters with the second method where estimates were used in performing the clustering.

When measuring variability of the independent components it is better to have corresponding components in one cluster rather than separate clusters. Also clear artifacts from a cluster can be filtered out later. Preferring clustering through the estimates to the single-link clustering is therefore a clear choice. Smaller clusters might vanish with that way and the single-link clustering will be better in detecting those clusters. The independent components are analyzed with the method that created 50 clusters.

### 4.2.2 ICA

The components of the different bootstrap runs were clustered to 50 clusters. From each cluster the probability of the activation appearing in each voxels was calculated. ICs thresholded at $p < 0.05$ were applied when counting the probabilities. Contours for probability of 50, 70, 80 and 90 percent were plotted. The corresponding colors were red, green, purple and black. Figures of the probabilities were plotted so that the maximum probability appears in every slice.

Real stable components were found in the auditory area and the visual processing areas. Also three clear artifact components appeared in almost every run the first in the verticles, the second in the brain stem and the third in the temporal pole. A stable component was also found in the association cortex. Temporally all independent components were stable caused by the Tensor-ICA which is partly temporal. The component in the auditory area in figure(13) located at almost the same place in every bootstrap run. This component was really stable spatially and temporally. Speech caused activation for this component however music did not cause any clear activation.

Another spatially stable component was in the visual processing area in the inferior division of the lateral occipital cortex (v5) shown in figure(14). It appeared in all but one run. As can be seen there is only little difference between 90 percent and 50 percent contours. Also other visual processing components having activation in over 80 percent of bootstrap runs were found. In these components the activation

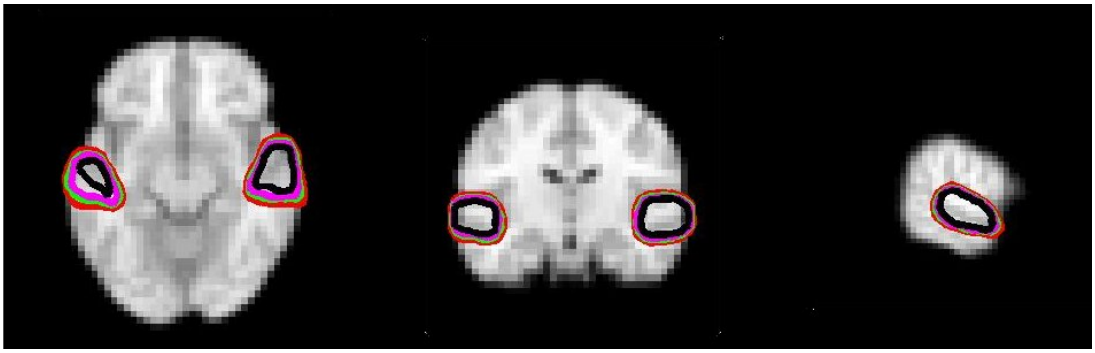

Figure 13: The contours of the auditory independent component that is activated during speech.

is wider spread and some runs did not contain these components at all. Components in the superior division of the lateral occipital cortex, the occipital pole, the supracalcarine and the cuneal cortex, the precuneous cortex and the lingual gyrus are shown in figures 15, 16, 17, 18 and 19.

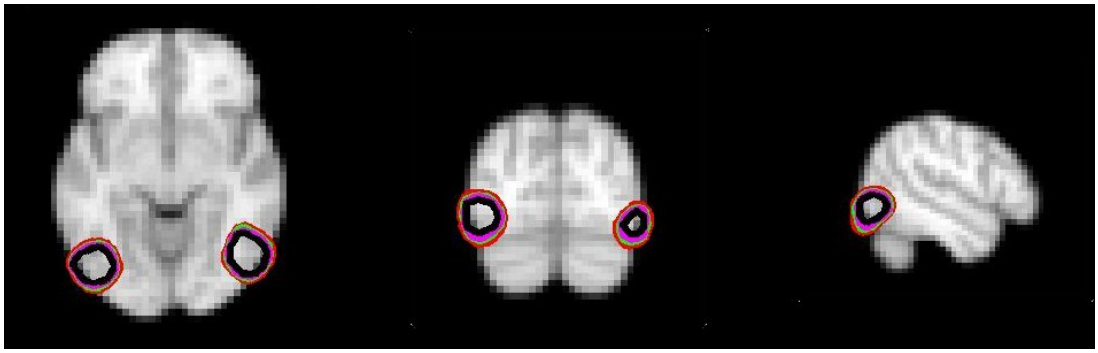

Figure 14: The visual proseccing component appearing near the visual prosessing area V5

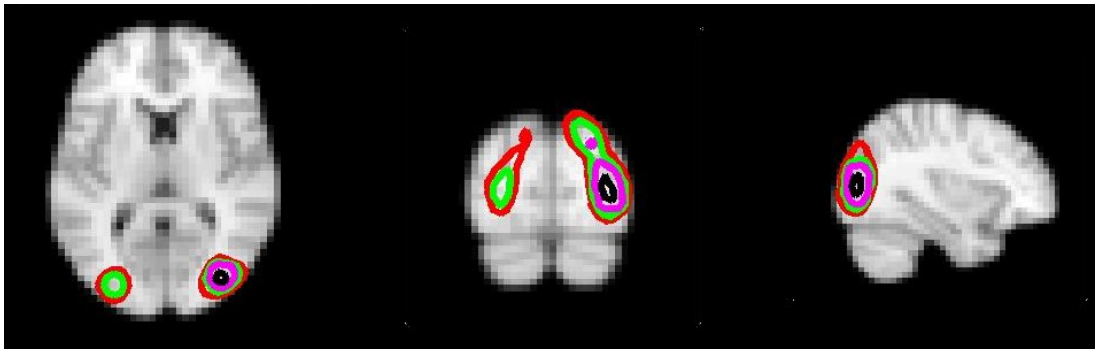

Figure 15: The independent component appearing in the superior division of the lateral occipital cortex

The independent component in figure(20) located in the superior parietal lobule appeared in 80 runs. Hand movements in the movie seemed to cause most of this component's activation peaks. Activation waged to the right side but in some components there was more activation in the left side. Both sides contained smaller areas of activation in the precentral gyrus in some runs forming a network from activations. The other component forming a network is found in the superior division of the lateral occipital cortex and the middle frontal gyrus figure(21). The third network is located in regions of the middle temporal gyrus, the precuneous cortex and the precentral gyrus shown in figure(22).

Near the auditory area in the middle temporal gyrus is a component which is probably related to language processing. This is a stable component as can be seen from figure(23) where the activation appears over 90 percent of the time in the same spatial location.

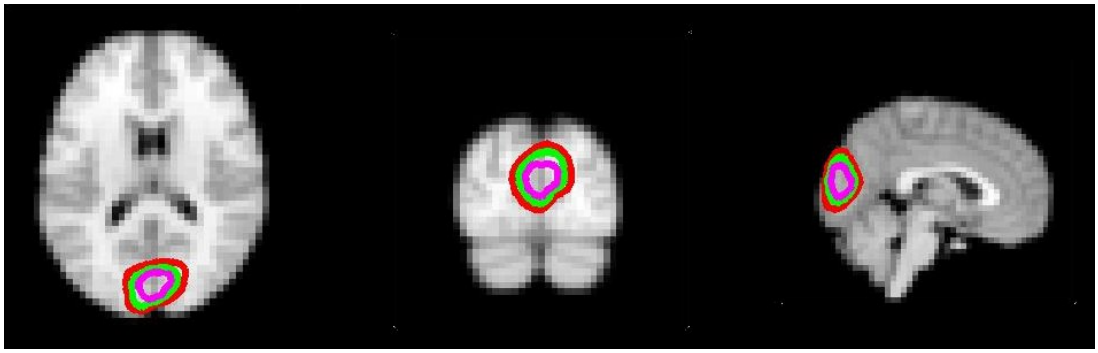

Figure 16: The independent component found in the occipital pole

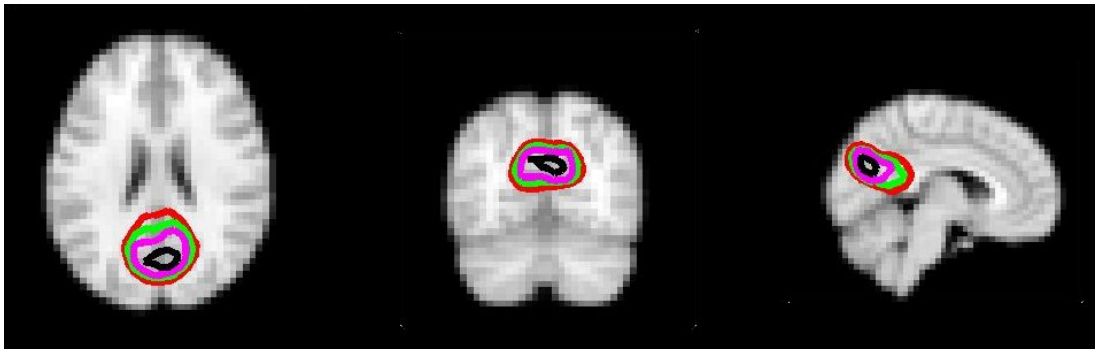

Figure 17: The independent component appearing in the supracalcarine and the cuneal cortex

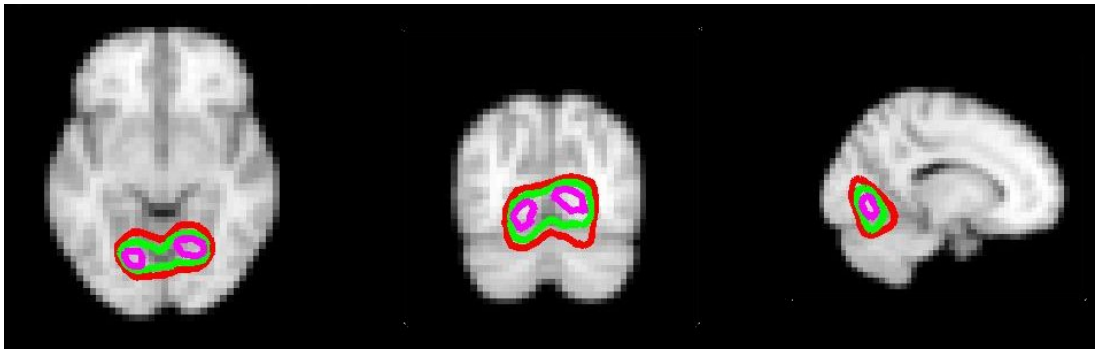

Figure 18: The independent component appearing in the precuneous cortex

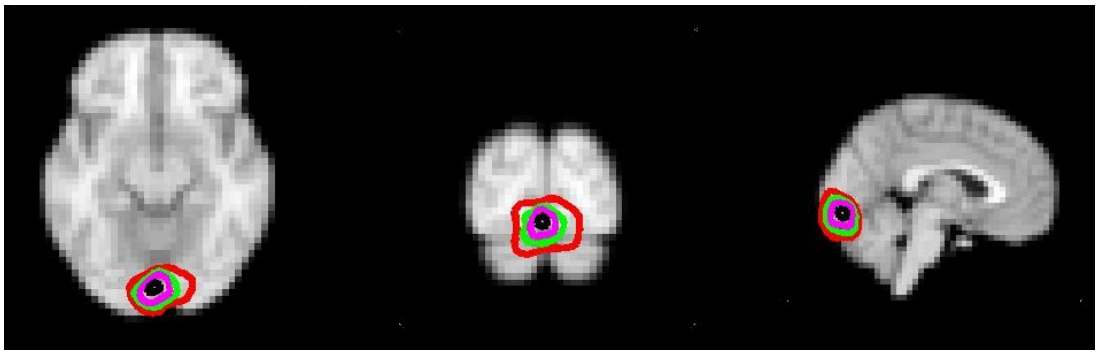

Figure 19: The independent component located in the lingual gyrus

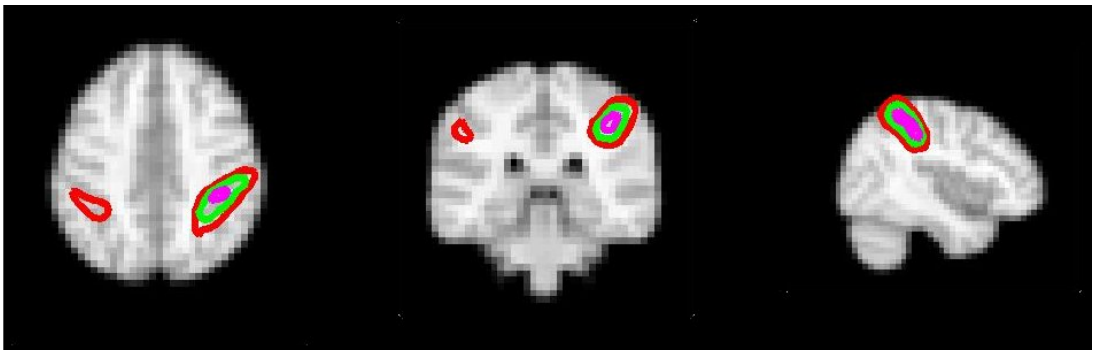

Figure 20: The independet component found in in the superior parietal lobule

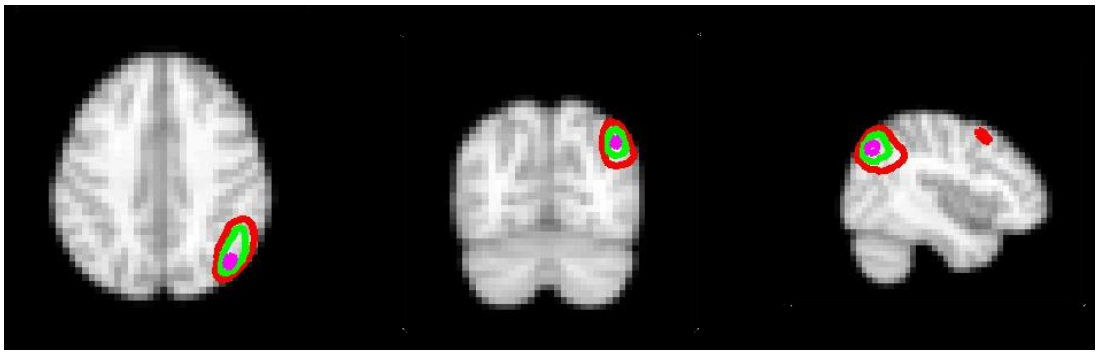

Figure 21: The independent component containing a network

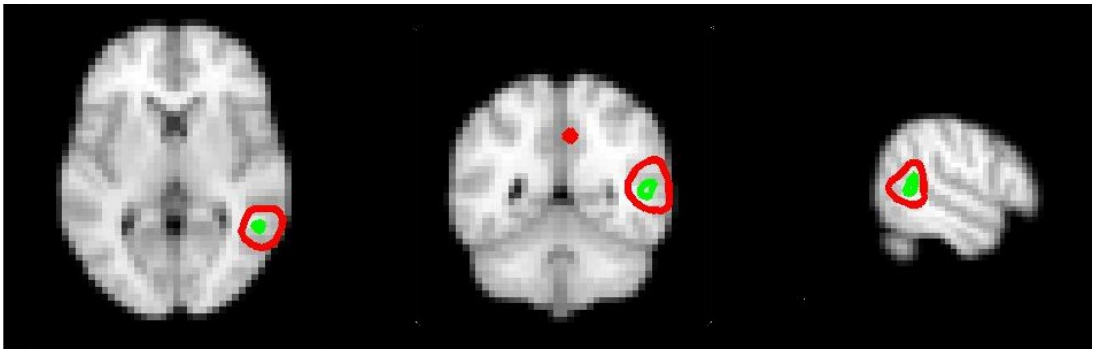

Figure 22: The independent component containing a network

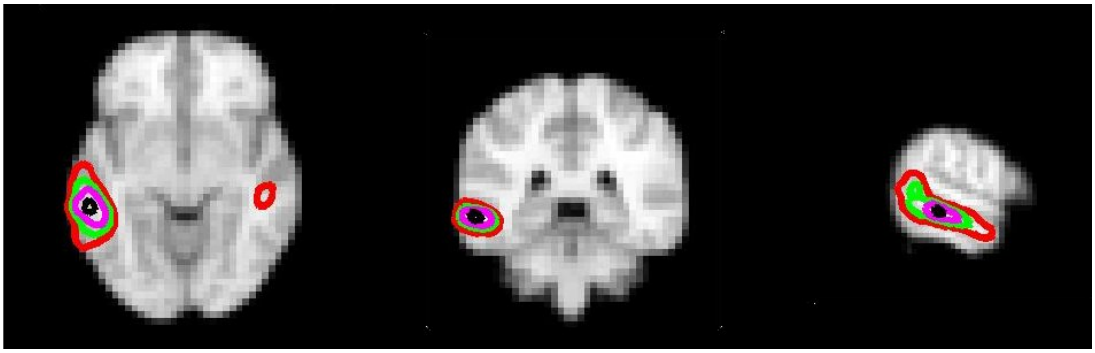

Figure 23: The stable component in the middle temporal gyrus

### 4.2.3 Temporal variability

Time series of the components in each cluster were plotted the same way as in figure(24). The times series is from the component shown in figure(22). The red line is the mean of all time series. The different tones of blue represent areas where 50, 75 and 100 percents of the time series are located. Many subjects react to a stimulus if the mean shows activation. When there is only activation in the quartile but the mean stays still this means that some subjects react to a stimulus in the movie but the rest do not.

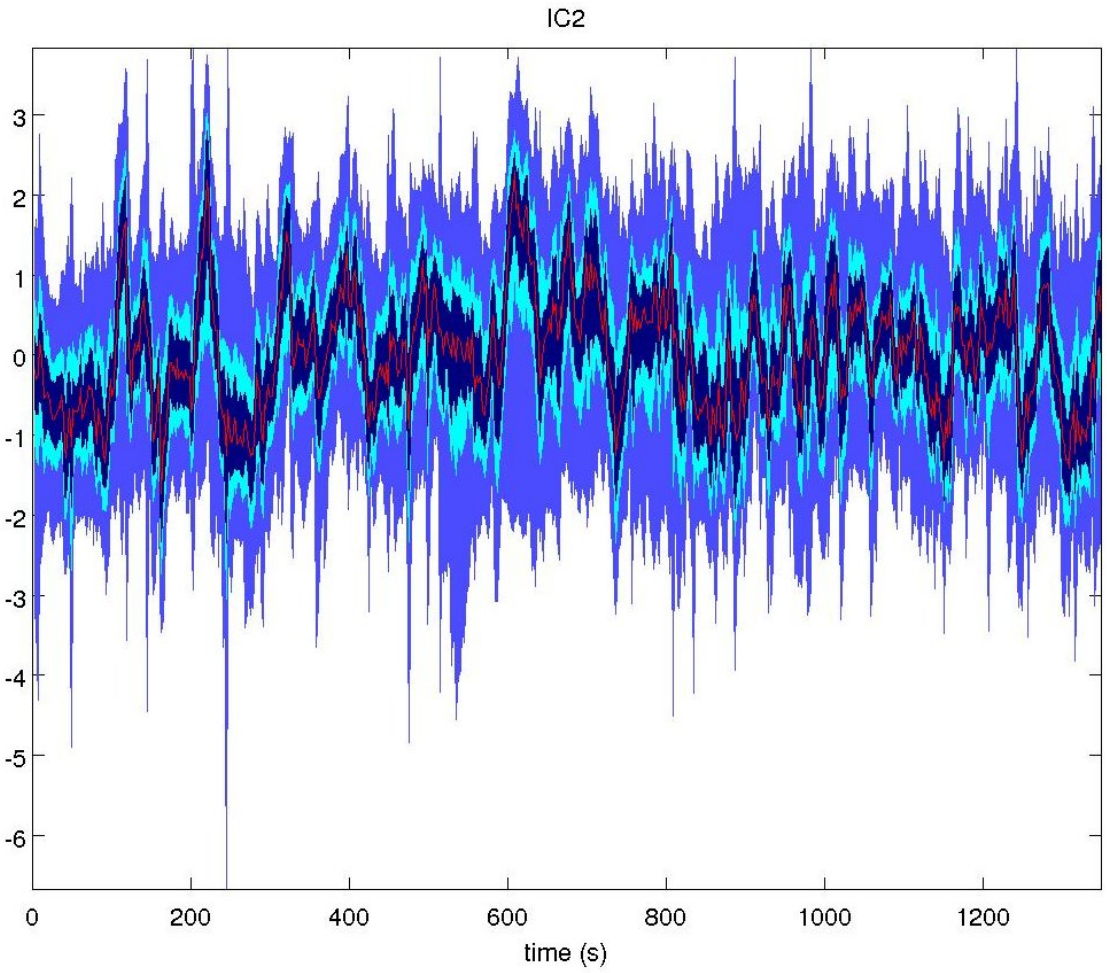


Figure 24: The time series represent areas where 50, 75 and 100 percents of the time series are located as different colors. The red line shows the mean.

Components found by the Tensor-ICA were temporally stable as the spread around the mean was large only in few time series in the cluster. The most stable was the auditory component where the time series of the bootstrap runs looked almost the same. The other components showed a little bit more variability. The temporal

consistency could be expected because Tensor-ICA is not completely spatial but is partly temporal.

## 4.3 Comparison of ICA and ISC

In ICA the point of activation can be seen more accurately than in ISC. As ISC is counted from several time points the activation of IC can be counted for every time point separately. From time series of IC many small changes in brain can be seen as ISC reacts to more explicit changes. This can be seen in figure(25) where time series of the independent component in the parietal area and the number of the same area's significant voxels from the intersubject correlation analysis are presented. There are more peaks in the IC time series represented in blue which are caused by some stimuli in the movie. These same stimuli are hard to find from the ISC time series and some do not appear at all.

When studying people watching a movie ISC finds the scenes that cause similar changes in every subject's brain region. With ICA it's possible to study more accurately events inside these scenes. ICA can also separate artifacts from the real signal and be used as a preprocessing stage for ISC analysis.

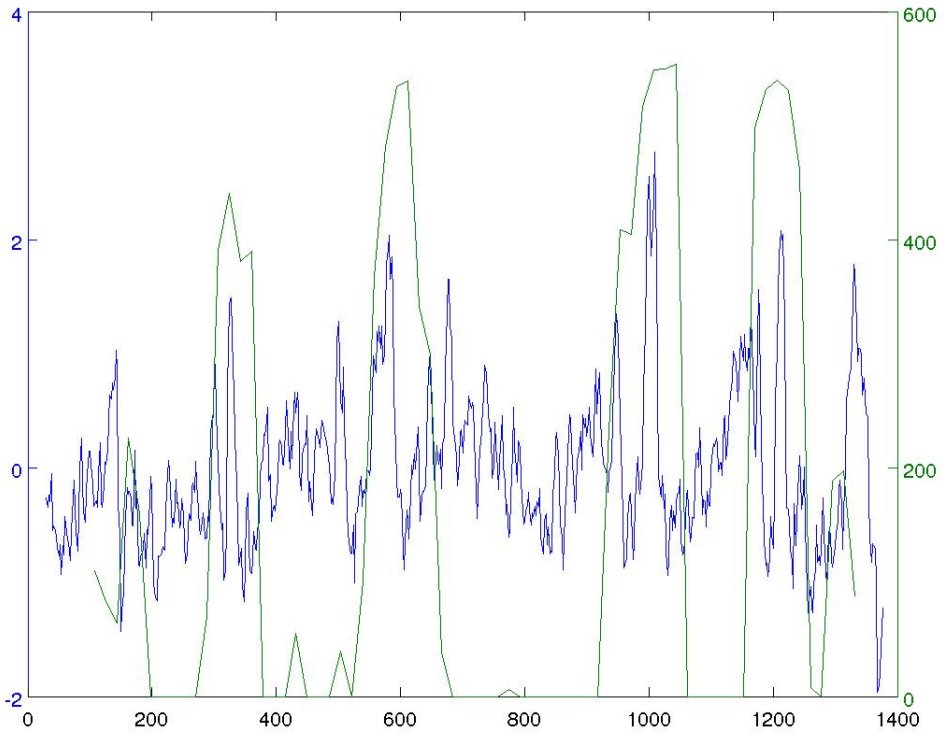


Figure 25: Time series of the independent component from the parietal area plotted in blue and the number significant voxels in the superior parietal lobule plotted in green.

# 5 Discussion

## 5.1 The study

The movie Tulitikkutehtaan tyttö was shown to 12 subjects. The movie should create a similar natural stimulus that occurs in human's everyday life. Brain activity of the subjects was measured by fMRI during the movie watching. The aim of the study was to find similar brain responses among all of the subjects and to examine the stimuli causing them.

The fMRI data was analyzed by the independent component analysis. The objectcs were to test the consistency of the independent components and to find the most consistent ones. This was studied by bootstrapping and clustering the data. Time series of the ICs were studied and compared to the scenes in the movie to find stimuli causing the components.

The intersubject correlation analysis was used to find the brain regions containing similar responses during the whole movie. ISC in different frequencies were explored by dividing the data to subbands. A common value for all pairwise intersubject correlations was calculated. The data was windowed and ISC was calculated to the windowed data to recognize the stimuli causing the correlation.

## 5.2 ICA

The movie as a stimulus caused many consistent independent components common to the subjects. As expected the experiment revealed two consistent independent components in the auditory processing area and few stable components in the visual processing area appearing in almost every bootstrap run. Some ICs where significant activation was in the same area in over 80 percent of the bootstrap runs were found in the parietal area and in the visual processing area. Some consistent components forming a network were also found. Significant brain activity was found in a wide area in almost every component. Three artifacts appeared in most of the runs meaning that the data contained some noise still after preprocessing. The timeseries of the spatially consistent components were stable.

A stimulus causing activity for two ICs could be found from the movie. Speech caused activation for the auditory component however music did not cause activation indicating that brain processes speech and music separately. Hand movement in the movie was found many times when there were peaks in time series of the component in the superior parietal lobule. This indicates that motoric stimulus like hand movements are processed in the superior parietal lobule. For other components clear stimuli could not be found. Here an annotation of the movie is needed to get a better idea of the other components' relation to the movie.

## 5.3 ISC

ICA was run to each subject separately and the artificial components found by ICA were removed from the original data. Intersubject correlations were calculated from

resulting data in fullband and in five subbands. In fullband significant correlation was found in the auditory and the visual processing areas as expected. There was also synchronization in the parietal areas.

The deviation of the data to five subbands revealed the dominance of the auditory and the visual processing areas in higher frequencies. These regions and the parietal areas showed synchronization in all subbands. In low frequencies significant correlation was also found in frontal parts of the brain.

The intersubject correlation was calculated to the windowed data in fullband. There were scenes in the movie where significant correlation could be found in many brain regions. During some scenes correlation could only be found in a few regions. There were also scenes where correlation could not be found in any part of the brain. Speech seemed to cause correlation in the auditory processing areas. Voxels in the superior parietal lobule correlated when stimuli related to working with hands are presented. Clear stimuli causing correlation in the other regions could not be found.

## 5.4 Future research

When ICs and ISCs are studied a good annotation of the movie is needed to get a better idea of the possible stimuli causing the brain responses. With ICA many artifacts can be found and removed from the data making future studies better. An automatic program to remove these artifacts would be rational to use. ISC can be calculated from the windowed data in different frequency bands. The window size must be designed so that they are reasonable for the frequencies. More movies have to be studied to confirm the findings from the study of Tulitikkutehtaan tyttö. New movies could be designed for the purpose of brain study. The findings from this study could be used in designing the forthcoming movies.

# References


[1] U. Hasson, Y. Nir, I. Levy, G. Fuhrmann, and R. Malach. Intersubject synchronization of cortical activity during natural vision. *Science*, 303(5664):1634, 2004.

[2] A. Bartels and S. Zeki. The chronoarchitecture of the human brainnatural viewing conditions reveal a time-based anatomy of the brain. *NeuroImage*, 22(1):419–433, 2004.

[3] I.P. Jääskeläinen, K. Koskentalo, M.H. Balk, T. Autti, J. Kauramäki, C. Pomren, and M. Sams. Inter-subject synchronization of prefrontal cortex hemodynamic activity during natural viewing. *The Open Neuroimaging Journal*, 2:14, 2008.

[4] D.W. McRobbie, E.A. Moore, M.J. Graves, and M.R. Prince. *MRI from Picture to Proton*. Cambridge Univ Pr, 2003.

[5] Aaron Filler. File:spin echo diagram.jpg. http://en.wikipedia.org/wiki/File:Spin_Echo_Diagram.jpg, July 2009.

[6] S.A. Huettel, A.W. Song, and G. McCarthy. *Functional magnetic resonance imaging*. Sinauer Associates Sunderland, MA, 2004.

[7] P. Jezzard, P.M. Matthews, and S.M. Smith. *Functional MRI: an introduction to methods*. Oxford University Press Oxford, 2001.

[8] M. Jenkinson, P. Bannister, M. Brady, and S. Smith. Improved optimization for the robust and accurate linear registration and motion correction of brain images. *Neuroimage*, 17(2):825–841, 2002.

[9] Kaveh Vahedipour. Juelich extensible mri simulator. http://www.jemris.org/jemris/doc/html/ug_JEMRIS_seq.html, September 2008.

[10] S. Clare. Functional MRI: methods and applications. *Online document], 9 Aug. 2000*, 2002.

[11] S.M. Smith. Fast robust automated brain extraction. *Human Brain Mapping*, 17(3):143–155, 2002.

[12] K.H. Höhne and W.A. Hanson. Interactive 3D segmentation of MRI and CT volumes using morphological operations. *Journal of Computer Assisted Tomography*, 16(2):285, 1992.

[13] B. Biswal, E.A. Deyoe, J.S. Hyde, et al. Reduction of physiological fluctuations in fMRI using digital filters. *Magnetic Resonance in Medicine*, 35(1):107–113, 1996.

[14] C.G. Thomas, R.A. Harshman, and R.S. Menon. Noise reduction in BOLD-based fMRI using component analysis. *Neuroimage*, 17(3):1521–1537, 2002.

[15] T. Kochiyama, T. Morita, T. Okada, Y. Yonekura, M. Matsumura, and N. Sadato. Removing the effects of task-related motion using independent-component analysis. *Neuroimage*, 25(3):802–814, 2005.

[16] V. Perlbarg, P. Bellec, J.L. Anton, M. Pélégrini-Issac, J. Doyon, and H. Benali. CORSICA: correction of structured noise in fMRI by automatic identification of ICA components. *Magnetic resonance imaging*, 25(1):35–46, 2007.

[17] J. Tohka, K. Foerde, A.R. Aron, S.M. Tom, A.W. Toga, and R.A. Poldrack. Automatic independent component labeling for artifact removal in fMRI. *Neuroimage*, 39(3):1227–1245, 2008.

[18] A. Hyvärinen and E. Oja. Independent component analysis: algorithms and applications. *Neural networks*, 13(4-5):411–430, 2000.

[19] A.J. Bell and T.J. Sejnowski. An information-maximization approach to blind separation and blind deconvolution. *Neural computation*, 7(6):1129–1159, 1995.

[20] C.F. Beckmann and S.M. Smith. Probabilistic independent component analysis for functional magnetic resonance imaging. *IEEE transactions on medical imaging*, 23(2):137–152, 2004.

[21] M.E. Tipping and C.M. Bishop. Mixtures of probabilistic principal component analyzers. *Neural computation*, 11(2):443–482, 1999.

[22] A. Hyvärinen. New approximations of differential entropy for independent component analysis and projection pursuit. *Advances in neural information processing systems*, pages 273–279, 1998.

[23] CM Bishop. Neural networks for pattern recognition. Clarendon, 1995.

[24] A.P. Dempster, N.M. Laird, D.B. Rubin, et al. Maximum likelihood from incomplete data via the EM algorithm. *Journal of the Royal Statistical Society. Series B (Methodological)*, 39(1):1–38, 1977.

[25] B.S. Everitt and E.T. Bullmore. Mixture model mapping of brain activation in functional magnetic resonance images. *Human Brain Mapping*, 7(1):1–14, 1999.

[26] R.A. Harshman and M.E. Lundy. The PARAFAC model for three-way factor analysis and multidimensional scaling. *Research methods for multimode data analysis*, pages 122–215, 1984.

[27] CF Beckmann and SM Smith. Tensorial extensions of independent component analysis for multisubject FMRI analysis. *Neuroimage*, 25(1):294–311, 2005.

[28] J-P Kauppi, I Jääskeläinen, M Sams, and J Tohka. Inter-subject correlation of brain hemodynamic responses during watching a movie: localization in space and frequency. *Frontiers in Neuroinformatics*.

[29] Y. Golland, S. Bentin, H. Gelbard, Y. Benjamini, R. Heller, Y. Nir, U. Hasson, and R. Malach. Extrinsic and intrinsic systems in the posterior cortex of the human brain revealed during natural sensory stimulation. *Cerebral Cortex*, 17(4):766, 2007.

[30] S.M. Wilson, I. Molnar-Szakacs, and M. Iacoboni. Beyond superior temporal cortex: intersubject correlations in narrative speech comprehension. *Cerebral Cortex*, 18(1):230, 2008.

[31] T. Nichols and S. Hayasaka. Controlling the familywise error rate in functional neuroimaging: a comparative review. *Statistical methods in medical research*, 12(5):419, 2003.

[32] Y. Benjamini and Y. Hochberg. Controlling the false discovery rate: a practical and powerful approach to multiple testing. *Journal of the Royal Statistical Society. Series B (Methodological)*, pages 289–300, 1995.

[33] Y. Hochberg and A.C. Tamhane. *Multiple comparison procedures*. Wiley New York, 1987.

[34] Y. Benjamini and D. Yekutieli. The control of the false discovery rate in multiple testing under dependency. *The Annals of Statistics*, 29(4):1165–1188, 2001.

[35] M.J. McKeown, S. Makeig, G.G. Brown, T.P. Jung, S.S. Kindermann, A.J. Bell, and T.J. Sejnowski. Analysis of fMRI data by blind separation into independent spatial components. *Human Brain Mapping*, 6(3):160–188, 1998.

[36] J. Ylipaavalniemi. *Variability of Independent Components in functional Magnetic Resonance Imaging*. PhD thesis, HELSINKI UNIVERSITY OF TECHNOLOGY, 2005.

[37] Oxford UK Analysis Group, FMRIB. Fmrib software library. http://www.fmrib.ox.ac.uk/fsl/, January 2010.

[38] J. Tohka, E. Krestyannikov, I.D. Dinov, AM Graham, D.W. Shattuck, U. Ruotsalainen, and A.W. Toga. Genetic algorithms for finite mixture model based voxel classification in neuroimaging. *IEEE Transactions on Medical Imaging*, 26(5):696–711, 2007.

[39] D.W. Shattuck, S.R. Sandor-Leahy, K.A. Schaper, D.A. Rottenberg, and R.M. Leahy. Magnetic resonance image tissue classification using a partial volume model. *NeuroImage*, 13(5):856–876, 2001.